Dominic Benford[1], Harvey Moseley[1] and Jonas Zmuidzinas[2]

[1] Observational Cosmology Laboratory, NASA/GSFC, Greenbelt, MD 20771

[2] Downs Laboratory, Department of Physics, California Institute of Technology, Pasadena, CA

E-mail: Dominic.Benford@nasa.gov
Harvey.Moseley@nasa.gov
jonas@submm.caltech.edu

Abstract.

Here we review the principles of operation, history, present status, and future prospects for the primary candidate detectors for Cosmic Microwave Background (CMB) polarization studies. The three detector types we will discuss are semiconductor-based bolometers, superconducting transition edge sensor (TES) bolometer, and Microwave Kinetic Inductance Detectors (MKIDs). All of these detector types can provide the sensitivity to permit background-limited measurements of the CMB, but the ultimate selection of detectors will be largely determined by the ease of production and reliability of large arrays of such detectors. This paper describes the present state of development of these detectors, efforts to integrate them into large arrays, and the detector system developments necessary to enable a space CMB polarization mission.

1. Introduction

The B-mode polarization of the CMB is espected to be a very weak signal; to put limits on the tensor to scalar ration of primordial fluctuations $R \sim 0.01$, we must measure a B-mode signal as small as $\sim 10^{-8}$ of the CMB power. The measurement of such a weak signal over the full sky requires arrays of 10^3 to 10^4 single mode background limited detectors with detective quantum efficiency (DQE) near unity operating for a year, with backgrounds dominated by the CMB itself. Beyond sensitivity, the performance requirements for the detectors, such as response time and the $\frac{1}{f}$ noise corner depend on the design of the experiment, so the ultimate selection of the"best" detector must wait for a system design.

At millimeter wavelengths, many optical functions of the instrument, such as beam formation and filtering, are being implemented in planar superconducting circuitry integrated with the detectors. Different groups are including these beam forming and spectral filtering elements into the focal plane elements [1–8]. The filtered radiation must be coupled into the sensor element for detection. In bolometers, the component which absorbs the power can be different from the sensor element and can be optimized separately, but must be thermally connected to it. The ultimate design of a focal plane for a space mission to measure CMB polarization is not known, but the design tools and production processes required to design it are largely in place.

In this paper, we will focus on the development of the sensor elements and the multiplexing systems required to read out these integrated focal planes. The planar superconducting microwave circuits required for beam forming and filtering are treated separately in this report. Here, we review the state of the art for three classes of detectors which are candidates for use in a CMB polarization mission. All three types can in principle be coupled to planar circuits. The ultimate choice of a detector type will depend on a number of things:

(i) Performance: The detector must provide background limited sensitivity and detective quantum efficiency near unity observing the CMB at relevant wavelengths.

(ii) Readout: The detector must be compatible with a low noise readout system which can be easily integrated with the array.

(iii) Practical issues:
   (a) Fabrication process for detector must be compatible with that of other focal plane elements.
   (b) Array should be simple to integrate into the optical system.
   (c) Power consumption should be low to be compatible with coolers.

In this report, we review the state of the art for superconducting transition edge sensors (TES) thermal sensors, semiconductor thermal sensors and microwave kinetic inductance detectors (MKIDs), which are sensitive to photon number. Since the field is changing rapidly, the choice of detectors will depend on the rate of development of the different detectors and multiplexing systems and the requirements of the specific instrument implementation, so this review should be seen as a progress report.

2. Transition Edge Sensor Bolometers for CMB Polarimetry

by Dominic Benford

2.1. Introduction

A superconducting transition-edge sensor (TES) bolometer is a highly sensitive detector of light that can resolve individual photons at energies above the near-infrared and can operate at all wavelengths between the radio and gamma rays. The TES is a thermal sensor that measures a total power rate or energy deposition by measuring with great precision the increase in the resistance of a superconducting material that is biased within the superconducting-to-normal transition region. Here I describe the technology, including a technical description, a description of its state of maturity, and discuss its benefits and disadvantages from a statistical and systematic viewpoint. I analyze the technological readiness level of this option (see attached description of NASA's TRL definitions), and of the cost and timescale that would be required for the community to bring the technology to TRL 5, which would be a level appropriate to respond to an Announcement of Opportunity for a satellite mission.

2.2. A Broad History of Bolometers

Going back into history, the bolometer can be said to have originated a very long time ago. Arguably, the Greeks[1] and Incas[2] understood how to extract heat from light, so perhaps bolometry has existed since antiquity. (The more pedantic might argue that, first of all, the above examples are not designed to measure the heat in light in any precise way, and hence the "-metry" portion of the term is invalid, and additionally, it appears likely that the ancients believed that mirrors and lenses could be used to ignite fires by capturing and concentrating fire received from the sun, hence implying that there was no concept at the time of measuring the heat content of light to begin with.) I will begin this didactic history of the bolometer by referencing Frederick William Herschel [9], who in the waning days of the 18th century figured out

[1] Archimedes is said to have used mirrors to concentrate sunlight onto Roman warships during the siege of Syracuse (214-212 BC) to have set them on fire; while the veracity of this story has long been in dispute, the Greeks were certainly aware of the heat content of sunlight, and this is mentioned by Aristophanes in his play The Clouds of 424 BC: "Good chance but you have noted / A pretty toy, a trinket in the shops, / Which being rightly held produceth fire / From things combustible – / A burning glass, / Vulgarly call'd" (translation of Thomas Mitchell, 1822).

[2] For instance, at the Feast of Raymi, a fire was ignited by using a concave metal mirror focused onto cotton wool; the failure of the sun, a key deity of the Incan religion, to ignite said fire was taken as an ill omen (see, e.g, History of the Conquest of Peru by William Prescott, 1855). In a fictional account (Prisoners of the Sun, 1949), Hergé suggests that the pyres of the executed might be ignited by mirror, thereby placing the responsibility for carrying out executions on the sun god.

that the infrared exists by means of no more simple equipment than a prism and a thermometer. Of course, the quantitative measurement of the solar spectrum was quite inaccurate since he was unaware of the change in dispersion with wavelength in the infrared, but the idea of using a thermometer to measure the total amount of energy in a beam of light was still pretty clever. This led, the better part of a century later, the scientific polyglot Samuel Pierpont Langley to invent the bolometer [10] for his investigations of the solar spectrum (a problem not fully solved during the intervening eighty years). His bolometer design is shown in Figure 1.

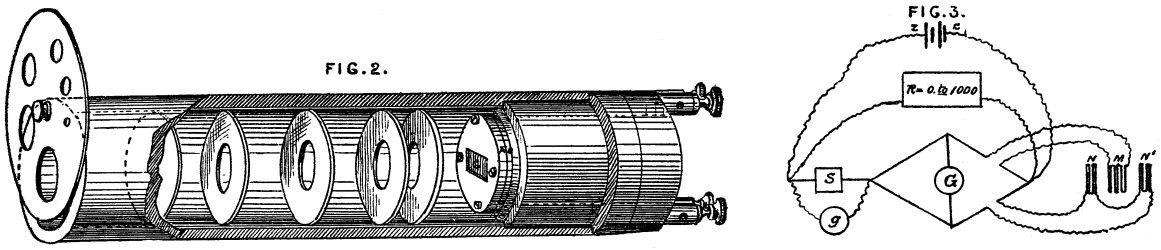

Figure 1. Bolometric instrument of S. P. Langley.

The next major advances in bolometry keep the core of Langley's original principles: an absorber converting light into heat, and a thermistor converting heat into an electrical signal. Superconducting bolometers made an early appearance, separately suggested by Goetz [11] and developed by Andrews et al. [12], with a composite structure consisting of a blackened aluminum foil absorber attached to a tantalum thermistor. It is of historical note that the Andrews group [13] found excess noise in their CbN (now known as NbN) superconducting bolometer for which they could ascertain no cause; this problem seems to plague researchers still today. However, no excess noise was reported in the more systematic study of Fuson [14] at the same institution. An important but logical improvement (see, e.g., Boyle and Rodgers' 4 K carbon resistor bolometer [15]) was made by Low [16] in 1961 by cooling the bolometer with liquid helium, increasing the sensitivity tremendously (by at least a factor of ten, from a noise equivalent power (NEP) of $\sim 5 \times 10^{-12}$ W/$\sqrt{\text{Hz}}$ [15] to $\sim 5 \times 10^{-13}$ W/$\sqrt{\text{Hz}}$ [16]). It is in 1977 that the term "transition edge" makes its way into the literature [17], with the seminal works of Clarke et al. [18] (Figure 2).

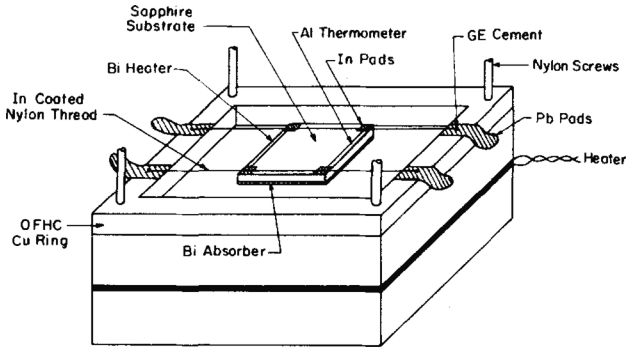

Figure 2. Superconducting bolometer demonstrated by Clarke et al. [17].

The idea of multiplexing large arrays of TES bolometers [19] goes back at least as far as 1990, although that line of research apparently ended shortly thereafter. The modern – an imprecise word, to be sure – TES bolometer period begins, in my opinion, with the mid-1990s work of the Berkeley group on voltage-biased superconducting bolometers [20], although the salient ideas

were presented first by Kent Irwin [21] for particle detection. I therefore end the history of superconducting bolometers in 1996.

No introduction to bolometers would be complete without at least some mention of the role of fabrication techniques and operational approaches. For instance, the idea of making bolometers by sputtering metals onto thin films has been around for at least eighty years [22]. A bolometer operating below the thermodynamic limit for 300 K radiation existed in 1946 [14]. Co-deposition of patterned thermistor and absorber films on substrates goes back at least forty years [23] . An array of bolometers – five pixels – was described by De Waard at the same time [24]. Pushing to subKelvin temperatures [25] brought another order of magnitude improvement in the noise equivalent power (NEP) of a factor of ten over the previous [16] work to $\sim 3 \times 10^{-14}$ W/$\sqrt{\text{Hz}}$. The concept of the monolithic bolometer – entirely produced by microlithographic techniques – was a breakthrough in 1984 by Downey et al. [26], although much of that had been done earlier [27]. Cooling bolometers with an adiabatic demagnetization refrigerator (ADR) was put forth by Britt and Richards in 1981 [28] with an eye to space flight use. The performance of a 200 mK bolometer was another two orders of magnitude better [29], at an NEP of $\sim 2 \times 10^{-16}$ W/$\sqrt{\text{Hz}}$. The Berkeley group proposed the TES-based hot electron bolometer [30] – an antenna-coupled device – which would provide a 100 mK NEP of $\sim 2 \times 10^{-18}$ W/$\sqrt{\text{Hz}}$, yet another two orders of magnitude and below the photon limit for most imaging applications except for the darkest sky in space.

There is also a wealth of historical discussion of the theory of bolometer performance. The WWII-era work of Milatz and Van Der Velden [31] on the noise components of bolometers is familiar even today. Billings et al. [32] worked out the sensitivity and temporal properties of metallic bolometers in 1947. The prolific R. Clark Jones developed explicit treatments for semiconducting bolometers [33] the ultimate sensitivity of Lambertian detectors [34], figures of merit for detectors [35], and culminating in his description of nonequilibrium bolometer performance in 1953 [36], three decades before the similar well-regarded work by John Mather [37]. This dynamic impedance view was extended by Y. Urano [38], who established a thermoelectric dynamic version resulting in stability predictions. At a similar time, investigations into superconducting bolometers pursued still-relevant topics such as the effect of bias current on bolometer behavior [39] and the excess noise on the transition [40]. An equivalent-circuit technique for superconducting bolometers was given by Maul and Strandberg [41], who were also involved in a noise-mitigation technique using external magnetic fields [42], and who claimed to have reached the thermodynamic limit by that means. Bertin and Rose [43] compared superconducting bolometers to the then-state-of-the-art semiconducting bolometers and concluded that superconducting bolometers were superior. Too bad this information was largely disregarded. An effort was made to model $1/f$ noise [44] and phase-slip shot noise [45] in bolometers. The award for not-quite-insightful-enough goes to the ironically-named Sherlock and Wyatt for their general analysis of self-heating in bolometers which mentioned in passing that for superconducting bolometers, the positive electrothermal feedback induced by the current bias could be reduced to near zero if the load resistor were set to a value of roughly the TES resistance [46].

2.3. A Brief Theoretical Description of the TES Bolometer

A very thorough discussion of the theory of TES bolometers, in particular derivations of or at least lists of relevant equations, has been written by Irwin and Hilton [47]. I will not try to reproduce that weighty tome here, but will rather summarize the equations using their notation to facilitate comparison. The linear differential equations for the electrothermal behavior of a TES bolometer are:

$$L\frac{\mathrm{d}I}{\mathrm{d}t} = V - IR(T,I) \text{ and } C\frac{\mathrm{d}T}{\mathrm{d}t} = P_{\text{bath}} + P_{\text{J}} + P, \tag{1}$$

where the electrical parameters refer to the inductance L, the Thevenin equivalent bias voltage V, the measured detector current I, the Thevenin equivalent bias load resistor R_{L}, and the TES resistance $R(T, I)$, and the thermal parameters are the heat capacity C and TES temperature T, P_{bath} is the power cooling the TES to the heat bath, P_{J} is the Joule power dissipation from the bias, and P is the optical signal power to be found. In detail, the resistance function depends on other physical variables such as the external magnetic field, but for simplicity it is easier to consider the constant-field case. The shape of $R(T, I)$ can be modeled theoretically and measured directly (Figure 3).

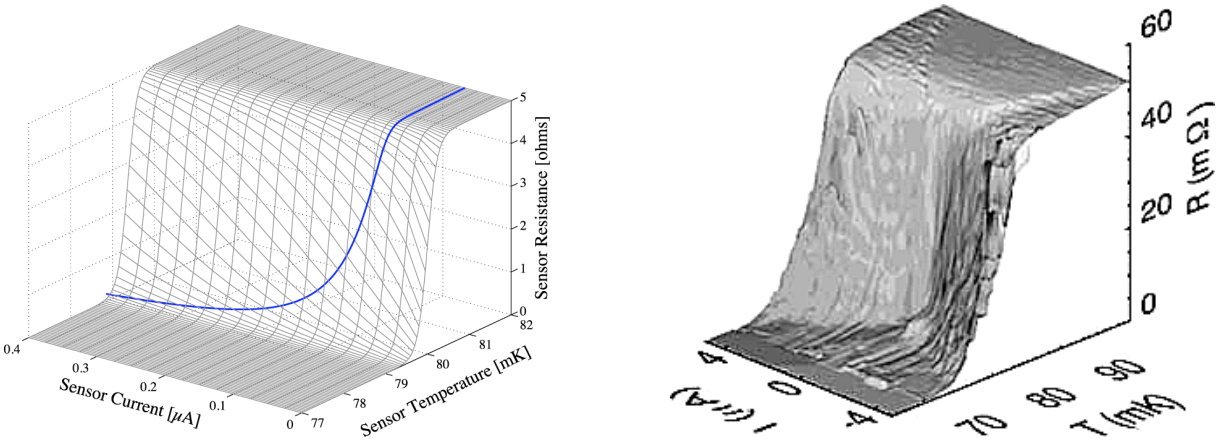

Figure 3. (Left) A modeled resistance function $R(T, I)$, showing the path followed during a bias sweep; adapted from a figure by Blas Cabrera [48]; (Right) Measurements of the $R(T, I)$ surface by Lindeman et al. [49], showing the shape of the transition in detail; note the similarity to the gross features of the model, given that the data have bipolar current.

The resistance can be expanded about nominal values of R, T, and I in the small-signal limit:

$$R(T, I) \approx R_0 + \frac{\partial R}{\partial T}\Big|_{I_0} \partial T + \frac{\partial R}{\partial I}\Big|_{T_0} \partial I \tag{2}$$

which has terms reminiscent of the dimensionless sensitivity of the resistance with temperature and current:

$$\alpha = \frac{T_0}{R_0}\frac{\partial R}{\partial T}\Big|_{I_0} \text{ and } \beta = \frac{I_0}{R_0}\frac{\partial R}{\partial I}\Big|_{T_0} \tag{3}$$

Substituting in a large number of similar small-signal approximations providing linear perturbations about equilibrium, the overall coupled differential equations relating the current and temperature to the voltage and power become:

$$\frac{\mathrm{d}}{\mathrm{d}t}\begin{bmatrix} \partial I \\ \partial T \end{bmatrix} = -\begin{bmatrix} \frac{1}{\tau_{\mathrm{el}}} & \frac{\mathscr{L}_I G}{I_0 L} \\ -\frac{I_0 R_0 (2+\beta_I)}{C} & \frac{1}{\tau_I} \end{bmatrix} \cdot \begin{bmatrix} \partial I \\ \partial T \end{bmatrix} + \begin{bmatrix} \frac{\partial V}{L} \\ \frac{\partial P}{C} \end{bmatrix} \tag{4}$$

where the variable τ_{el} and τ_I refer to the electrical and thermal time constants, respectively, and the DC loop gain $\mathscr{L}_I$ under constant current I is given by:

$$\mathscr{L}_I = \frac{P_{\mathrm{J}_0} \alpha_I}{G T_0} \tag{5}$$

Solving Equation 4 and integrating yields two eigenvalues for the reciprocal of the time constants involved in the TES bolometer response:

$$\frac{1}{\tau_+} = \frac{1}{2\tau_{\rm el}} + \frac{1}{2\tau_I} + \frac{1}{2}\sqrt{(\frac{1}{\tau_{\rm el}} - \frac{1}{\tau_I})^2 - 4\frac{R_0}{L}\frac{\mathscr{L}_I(2+\beta_I)}{\tau}} \tag{6}$$

$$\frac{1}{\tau_-} = \frac{1}{2\tau_{\rm el}} + \frac{1}{2\tau_I} - \frac{1}{2}\sqrt{(\frac{1}{\tau_{\rm el}} - \frac{1}{\tau_I})^2 - 4\frac{R_0}{L}\frac{\mathscr{L}_I(2+\beta_I)}{\tau}} \tag{7}$$

When a varying power is applied to a bolometer, the measured response will follow the power, but with a responsivity that varies with frequency according to the two poles defined by the time constants in Equations 6 and 7. If a small, sinusoidal power is applied to the bolometer, the solution to Equation 4 can be explicitly solved, and contains the time constants τ_+ and τ_-. Resubstituting, one can derive the small-signal response in current to a given power:

$$s_I(\omega) = -\frac{1}{I_0 R_0}\left[\left(\frac{L}{\tau_{\rm el} R_0 \mathscr{L}_I}\right) + \left(1 - \frac{R_I}{R_0}\right) + i\omega\frac{L\tau}{R_0\mathscr{L}_I}\left(\frac{1}{\tau_I} - \frac{1}{\tau_{\rm el}}\right) - \frac{\omega^2\tau}{\mathscr{L}_I}\frac{L}{R_0}\right]^{-1} \tag{8}$$

Typically, a TES bolometer is run with a strong voltage bias ($R_{\rm L} \ll R_0$) and strong electrothermal feedback (high $\mathscr{L}_I$), and so the DC responsivity simplifies to:

$$s_I(0) = -\frac{1}{I_0 R_0} \tag{9}$$

In a similar fashion to the above, the complex impedance of a TES bolometer can be calculated from Equation 4 by applying a voltage $V(\omega)$ and a response current $I(\omega)$. The result is a total circuit impedance of

$$Z(\omega) \equiv \frac{V(\omega)}{I(\omega)} = R_L + i\omega L + R_0(1+\beta_I) + \frac{R_0\mathscr{L}_I}{1-\mathscr{L}_I}\frac{2+\beta_I}{1+i\omega\tau_I} \tag{10}$$

which features the impedance of the bias circuit and the TES, and hence we can write

$$Z_{\rm TES}(\omega) = R_0(1+\beta_I) + \frac{R_0\mathscr{L}_I}{1-\mathscr{L}_I}\frac{2+\beta_I}{1+i\omega\tau_I} \tag{11}$$

In addition to the performance parameters above, a prediction of the noise of a TES bolometer is an absolute necessity. This has been done by many in the past, and Kent Irwin has added a nonlinear, nonequilibrium, first and second order calculation [50] to the existing theory [47]. The total noise is a combination of the thermal fluctutation noise in the bolometer thermal isolation, Johnson noise in the thermistor, noise from the bias circuit, noise from the readout amplifier, and excess noise arising from one or more of a variety of potential nonideal performance aspects. In this order, the total noise is:

$$\begin{aligned} S_{\rm total}(\omega) =& 4k_{\rm B}T_0^2 G F_{\rm thermal} + 4k_{\rm B}T_0 R_0 I_0^2 (1+2\beta_I)\frac{1+\omega^2\tau^2}{\mathscr{L}_I^2} + \\ & 4k_{\rm B}T_0 R_L I_0^2 \frac{(\mathscr{L}_I - 1)^2}{\mathscr{L}_I^2}\left(1+\omega^2\tau_I^2\right) + \frac{S_{I_{\rm amp}}}{|s_I(\omega)|^2} + S_{\rm Excess}(\omega) \end{aligned} \tag{12}$$

The thermal link function $F_{\rm thermal}$ can be calculated in the specular phonon or scattered phonon limit for a thermal link with temperature dependence T^n [51]:

$$F_{\rm thermal} = \frac{\left(\frac{T_{\rm bath}}{T_0}\right)^{n+2} + 1}{2} \text{ (specular) or } F_{\rm thermal} = \frac{n+1}{2n+3}\frac{\left(\frac{T_{\rm bath}}{T_0}\right)^{2n+3} - 1}{\left(\frac{T_{\rm bath}}{T_0}\right)^{n+1} - 1} \text{ (scattered)} \tag{13}$$

The thermal link function represents the behavior of fluctuations in a thermally isolating structure where a significant conductivity gradient exists across the structure. The conductance G is calculated at the warm end (T_0), and hence F_{thermal} reaches a maximum of unity at that point.

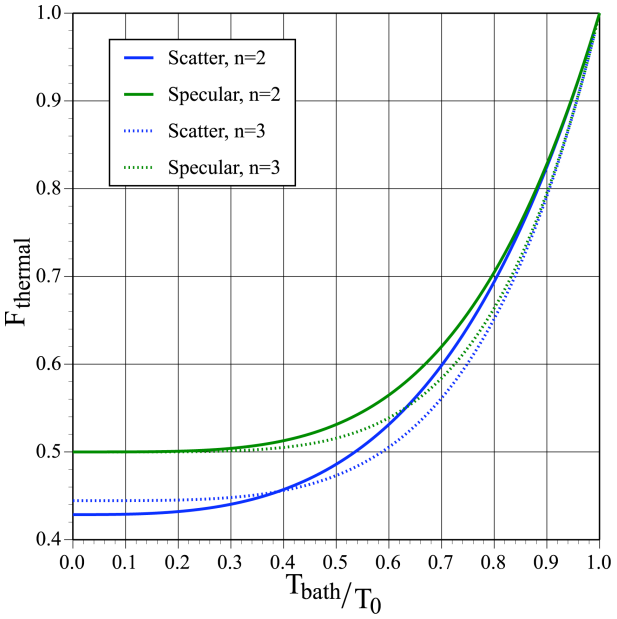

Figure 4. Thermal link functions as given by equations for specular- or scattering-dominated links in Dan McCammon's review [51].

Figure 4 shows the functional dependence for a reasonable range of the thermal conductivity index n. In Equation 12, there are two analytic unknowns. One is the amplifier noise, which, while it can be subjected to some amount of analysis, is more likely to be a quantity of known (measured) value in current noise units, hence the notation $S_{I_{\text{amp}}}(\omega)$. The other is a quantity of excess noise in power units $S_{\text{Excess}}(\omega)$. This is a subject of much investigation, and will be summarized later.

2.4. State of Maturity of TES Bolometer Development (or, how did we get here?)
My thesis advisor, Tom Phillips, once told me that the best papers to write are those that are the first in their field or those that are the last in their field. In keeping with this notion, and in the earnest expectation that the last papers on TES bolometer aspects are far from written, this section will summarize developments in TES bolometers in the first decade following the advent of the voltage-biased approach, what I will term the Decade of Development.

Since the Berkeley group introduced the voltage-biased superconducting bolometer [20] (although with a nod to Stanford [21]), this is a good point of departure to discuss the decade of 1996-2006. Their early efforts led to useful theory and experiment in the strong-feedback limit [52]. They also introduced a TES bolometer manufactured entirely with photolithography [53] – see Figure 5 –a step forward in fabrication technique that enables very large format arrays – which turned out to be the next thing they demonstrated, although only mechanically [54]. This same trio of authors also developed a theoretical treatment of the excess thermal fluctuation noise arising from undercoupled or distributed heat capacities on the bolometer [55].

The Stanford group achieved one early and notable milestone: the first astronomical application of TES bolometers. Using a small number of tungsten TES hot electron bolometers, Romani et al. [56] used photon-counting pixels that produced arrival time ($\delta t = 100\ ns$) and energy ($\delta E_\gamma \leq 0.15\ eV$) resolved measurements of the Crab pulsar from the near-IR through the near UV. This result is such a good indicator of the novel aspects of TES bolometers that it

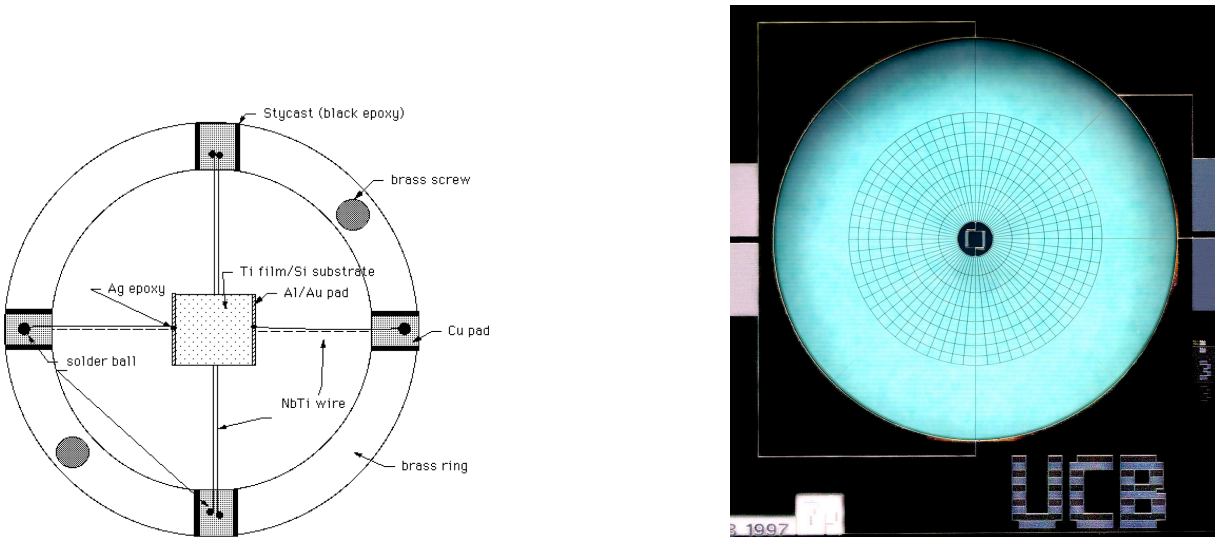

Figure 5. (Left) The layout of an early voltage-biased superconducting bolometer (e.g., [20]) is reminiscent of that in Figure 2 . (Right) The all-lithographic version (e.g., [53]) made large-format arrays possible.

represents an entirely new (although not CMB-related) approach to astronomical observations. Figure 6 shows the resultant photon count rate vs. phase and wavelength. As an aside, it

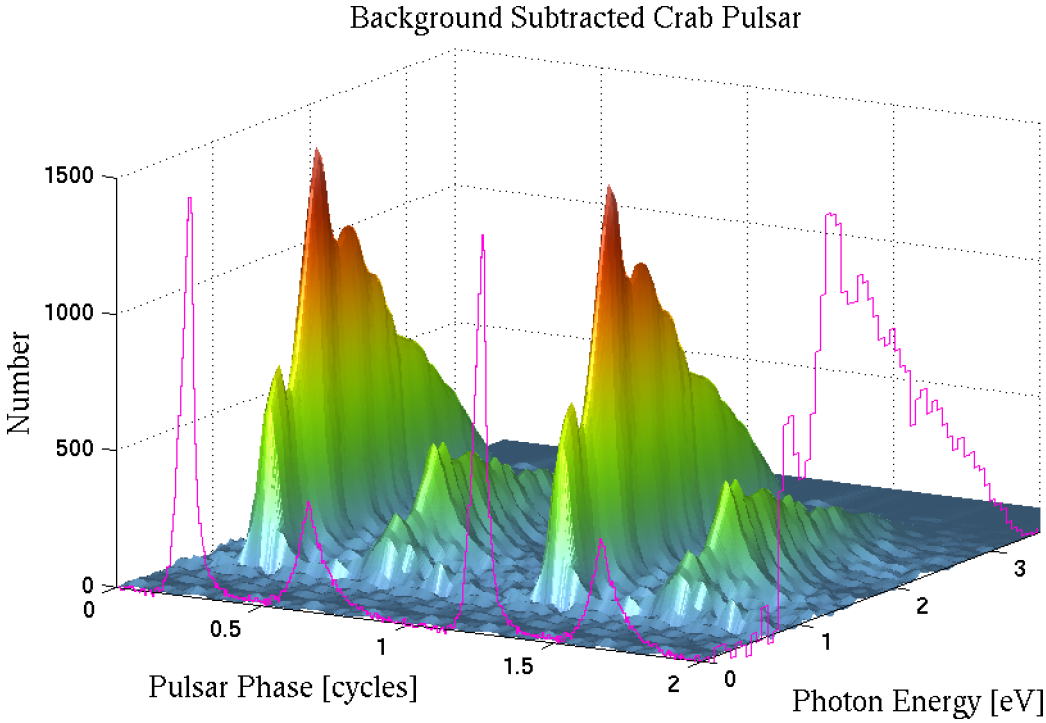

Figure 6. The first astronomical application of TES bolometers was to measure the brightness of the Crab Pulsar as a function of wavelength and phase [56].

is worthy of mention that this may be the only astronomical instrument yet fielded using

TES bolometers without a multiplexed SQUID readout. The NASA/GSFC group has been developing TES bolometers for long wavelength purposes since 1998 [57], in strong collaboration with NIST/Boulder. Developments intended for Herschel resulted in the first demonstration of a TES bolometer system operating using SQUID multiplexers [58] including the optical detection of light while multiplexing. Staguhn et al. [59] demonstrated that TES bolometers could be used with SQUID multiplexers and still retrieve Johnson-noise-limited readout. Later, ongoing efforts resulted in a robust design for near-phonon-noise-limited bolometers [60, 61]. Benford et al. fielded the first astronomical instrument using multiplexed TES bolometers [62]and produced the first astronomical images using an array of multiplexed TES bolometers [63]. This is shown in Figure 7, since it may be the first astronomical demonstration relevant to CMB polarimetry.

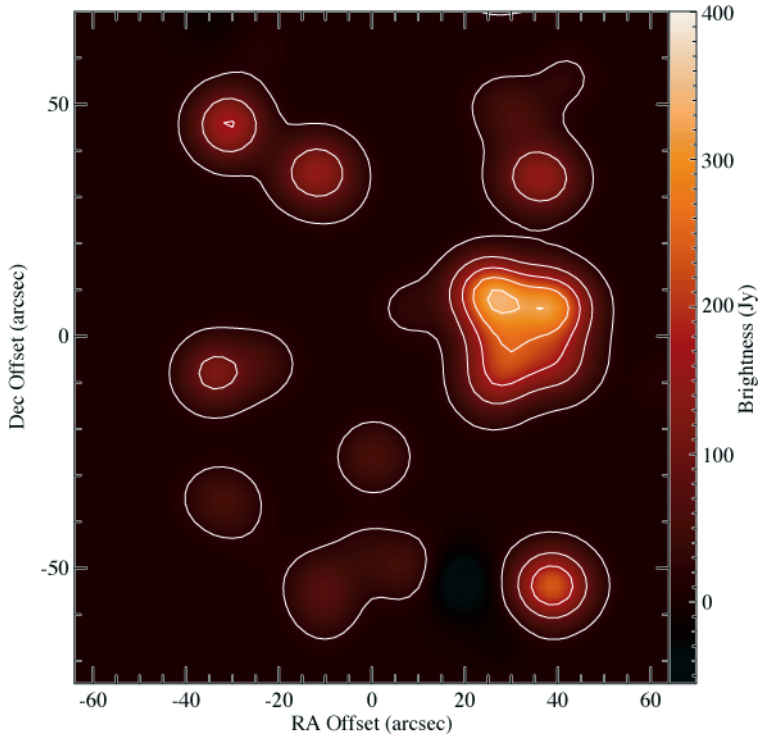

Figure 7. TES bolometer array 350 m image of the high-mass star formation region G34.3+0.2 (Benford et al. [63]).

The closing of the Decade of Development at Goddard was summarized by the realization that the TES capability available at the close of 2005 was robust enough to pursue astronomical instruments, rather than technology developments. In Section 4, I will cover the issue of technology readiness level – but in advance, I note that this decision marked the completion of TRL 4 ("Component and/or breadboard validation in laboratory environment"). A separate group at Goddard engaged in the development of TES-based X-ray microcalorimeters pursued the precise measurement and theoretical understanding of detector parameters. These can be typified by, for example, the interesting plot of $\beta(V)$ by Saab et al. [64], the hinting-at-some-underlying-physics of the excess noise vs. resistance of Lindeman et al. [65] and the optimization modeling of Bandler et al. [66].

NIST/Boulder has had a strong history in the SQUID multiplexers used by many groups, in particular the time-domain devices that have been incorporated into past and ongoing instrument developments. As a result, most of their focus was on the maturing of the readouts, resulting in the 8-element [67] 32-element [68], and 1,280-element [69] time domain SQUID

multiplexers. They also investigated the excess noise problem in TES bolometers using both geometry (in conjunction with NASA/GSFC [70]) and magnetic fields to mitigate the effect [71].

In contrast to the statement a few paragraphs ago, the Decade of Development did see the beginning of several TES-based millimeter-wavelength instruments. One of them was developed at the University of Pennsylvania, a 3 mm camera for the Green Bank Telescope [72] started under the name "Penn Array Receiver." (At the time of first observations, it was renamed to MUSTANG, but that was a later event). This camera is based on an 8×8 TES array [73] in a fully planar, close-packed format – the first such array designed for long wavelength astronomy. At the same time, the Princeton group began work on the Atacama Cosmology Telescope [74], which featured a three-band camera in the millimeter wavelength range. In a far-reaching vision, each band would feature a 32×32 array for true multikilopixel operation [75], based on the NASA/GSFC pop-up-detector architecture [76]. During the middle part of the 2000s, detector array development and, perhaps more importantly, detector system development proceeded on these two instruments. However, it was a time of much promise and little actual use of TES arrays in actual astronomical applications.

At Caltech/JPL, attention to TES bolometers started late (in part because of that august institution's well-established semiconducting bolometer array work receiving the majority of the focus), and so their most notable contribution – and quite relevant to CMB polarimetry – concerns antenna-coupled TES bolometers. One notable example is a membrane-isolated TES bolometer coupled via a microstrip to a twin-slot antenna [77]. While not strictly TES-related, the wideband or dual-polarization antenna networks of Goldin et al. [78] have definite application to them, as a TES version appeared the following year [79].

I will close this section with a return to the Berkeley group, who in addition to pursuing technology development (e.g., their own twin-slot TES bolometer [80], took the first step into the next generation: large-scale engineering of TES bolometer arrays. Their APEX-SZ camera achieved first light during an engineering run in December 2005 [81], with a small fraction of their bolometer complement (13%) operational. This instrument features monolithically-fabricated superconducting TES bolometer arrays in a hex-packed spiderweb geometry, read out by frequency-domain SQUID multiplexers. The first light results (Figure 8) point the way to mature, kilopixel-scale TES instruments, and are therefore a suitable closing to the Decade of Development of the TES bolometer.

2.5. Recent Papers and Developments (or, here is where we are.)

2.5.1. TES Excess Noise and Geometry Over the last few years, the quantification of "excess noise"[3] has become a burgeoning field. One source of such, "β noise" [82], is a consequence of rigorous nonequilibrium theory [50], and manifests as an increased Johnson noise. A similar but unrelated "β noise" is postulated by Ullom [71], but not duplicated by Hoevers [83]. Instead, they consistently find an effective white voltage noise [84, 85] Other noise sources include phase slip shot noise or flux-flow noise [86, 87], percolation noise [88], internal thermal fluctuation noise (ITFN) [52, 89], and the rather empirical-sounding fluctuation superconductvity noise [90] A technique for reducing ITFN (high resistivity TES with high conductivity substrate) appeared also to suppress the white voltage noise [91]. This makes it seem like a valid source of noise. On the other hand, an analysis on several points led Brandt et al. to conclude that both phase slip and percolation noise are present [92]. The detailed thermal models of Kinnunen et al. show that white noise and ITFN are both present [93]. As an assignment to reflect on, note that the electron-phonon-decoupling device of Barrentine et al. [94] might show no excess noise and, more importantly, a virtually featureless spectrum from 10 Hz – 1 kHz. Several groups have

[3] I shall continue to use this term despite what Kent Irwin said in 2006 [50], tongue presumably lodged firmly in cheek, that there is no such thing as excess noise, just "noise" and the ratio between it and what you expected.

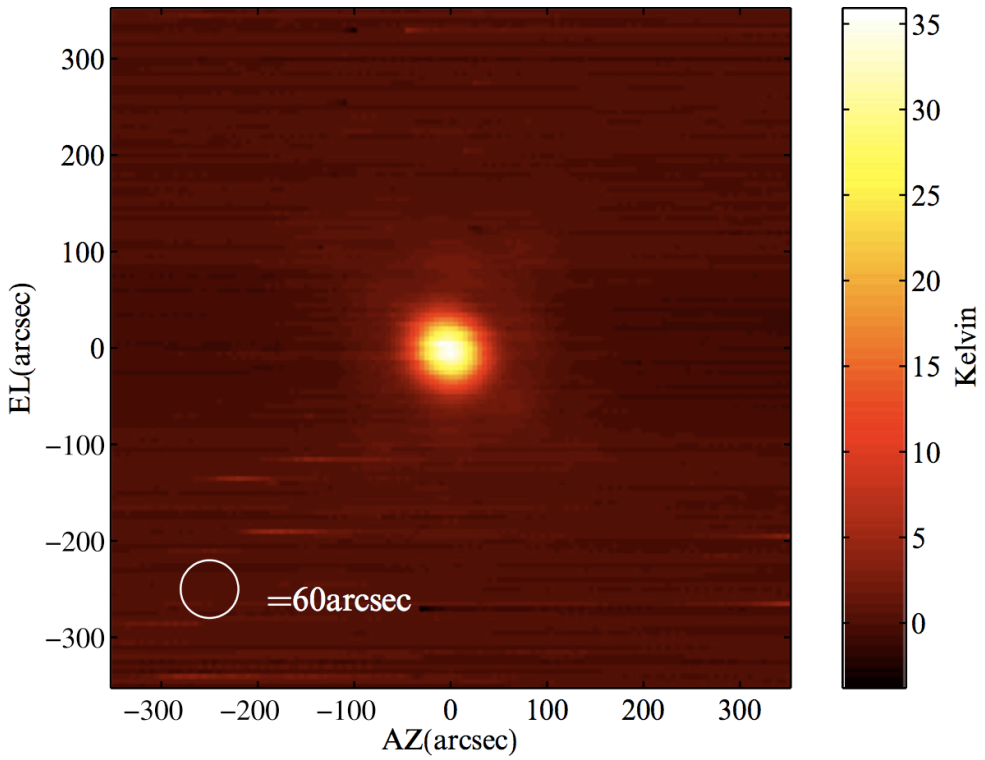

Figure 8. TES bolometer array 2 mm wavelength image of Jupiter using APEX-SZ (from Dobbs et al. [81]).

approached the excess noise as a geometrical problem. In this view, the reason(s) for the noise can all be reduced to a TES geometry problem, such as edge effects, percolation state space, etc. Adding or changing boundary conditions such as normal metal bars, stripes, or dots can change these effects and influence the excess noise. Among the first efforts of this sort were bars and stripes [60, 61, 71]. Dots are preferred by others [85]. A very clever circular geometry[4] has been in use for several years [95]. All of these appear to have excess noise, and where it is suppressed, other detector parameters have also changed. I would therefore conclude that to first order, geometry is not the determining factor in excess noise. In summary, while there are many competing and apparently valid (both theoretically and experimentally) models for the "excess noise", the only robust conclusion that can be drawn is that what gives rise to it is a poorly understood function of many (perhaps hidden) variables in the design of a TES bolometer.

2.5.2. Antenna-coupled devices Antenna-coupling provides a convenient method for controlling the solid angle of response of a TES bolometer, and hence limits the stray light it receives. There are additional benefits that can be realized in packaging (such as space to run wiring), although a price is paid relative to the efficiency of a filled array for wide-field mapping [96]. The simplest antenna-coupled TES bolometer array would be the effective equivalent of a bow-tie antenna array [1], but more sophisticated approaches are possible. Waveguide coupling includes feedhorns that can significantly improve the sidelobe response [2, 3]. The microstrips that are

[4] While I have called it a circular geometry, it is in fact annular. Due to its relation with the geometry of the Corbino effect (the Hall effect in a circular plate, named for Orso Mario Corbino), this is referred to as the Corbino TES geometry.

often used in an antenna-coupled TES bolometer can be used to define the wavelength response in an array, even allowing multicolor arrays [4] Alternatively, the microstrip can be used to combine the power of multiple antennas, such as in making a beam-forming antenna in two polarizations [5, 6]. Or, in a more integrated approach, functions such as polarization switching, band defining, and beam defining can be achieved simultaneously[7, 8].

The figures of merit for arrays of antenna-coupled TES bolometers are fairly straightforward. Depending on which of these functions are being defined by the antenna-coupling approach, they include: the repeatability of band definition and out-of-band suppression; the forward efficiency and sidelobe rejection of the spatial response function; the degree of cross-polarization and its repeatability; and the efficiency of using on-chip polarization modulation as opposed to full aperture modulation. For each approach, there is an increasing maturity of the numerical techniques for predicting antenna-coupled performance, but there is as yet a dearth of well-analyzed experimental effort on large data sets to extract the precise proof of their function.

2.5.3. Sensitivity Given the brightness of the CMB, it could be claimed that the sensitivity of the TES bolometer is not a technologically challenging aspect. This is, of course, a relative measure as compared to the sensitivity required for the detectors on a cryogenic space telescope operating at wavelengths of around 200-400 μm. A calculation of the components contributing to sky brightness in near-Earth space is shown in Figure 9, along with an estimate for the optical power and photon NEP that would be likely for a CMB polarization experiment in space. The NEP requirement for a CMB polarization detector is around 2×10^{-18} W/$\sqrt{\text{Hz}}$. Prototype far-infrared TES bolometers such as those for SAFIRE with an NEP requirement of 10^{-19} W/$\sqrt{\text{Hz}}$ [97], BLISS [98] on SPICA with a best NEP of $\sim 6 \times 10^{-20}$ W/$\sqrt{\text{Hz}}$ [99], SAFARI on SPICA with an NEP of $\sim 10^{-18}$ W/$\sqrt{\text{Hz}}$ [100], and even technology developments for the SAFIR observatory with an NEP approaching 10^{-20} W/$\sqrt{\text{Hz}}$ [101, 102].

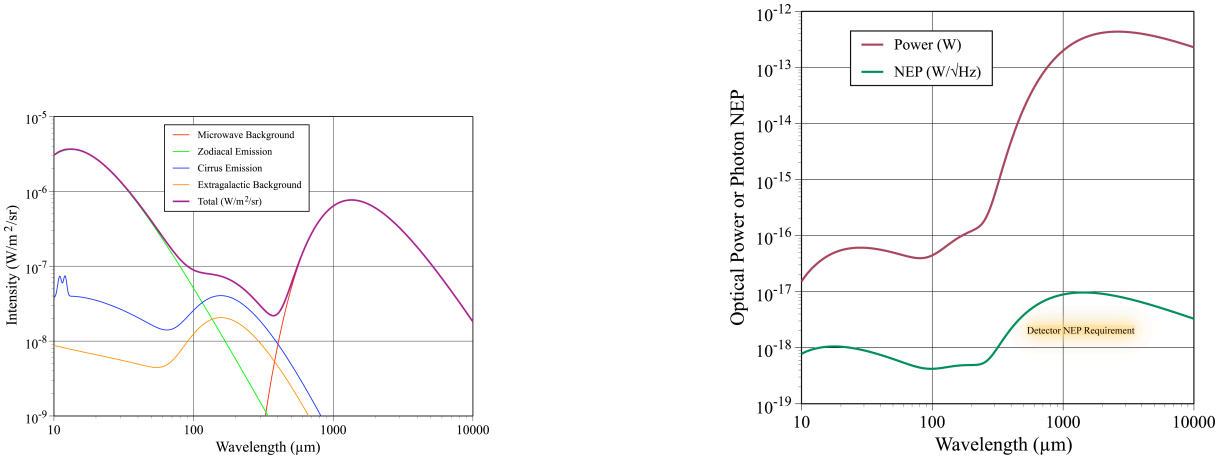

Figure 9. (Left) The calculated components of the celestial background shows that the CMB bands are significantly brighter than the far-infrared bands, and so sensitivity will be driven by far-IR instruments. (Right) A calculation of the optical power and photon NEP for a representative CMB polarization mission shows that the detector NEP requirement is not extreme.

2.5.4. Instruments As mentioned above, the Atacama Cosmology Telescope features in its Millimeter Bolometer Array Camera [103] one of the largest TES array sets currently in production or in use. Featuring three arrays of 1,024 pixels each, it has only recently been

operated in its complete configuration. At the time of this writing, the first light images consisted only of the data from one array (145 GHz) [104] from late (October-December) 2007. A photo of an ACT array and a map of the Sunyaev-Zel'dovich effect in the Bullet Cluster are shown in Figure 10.

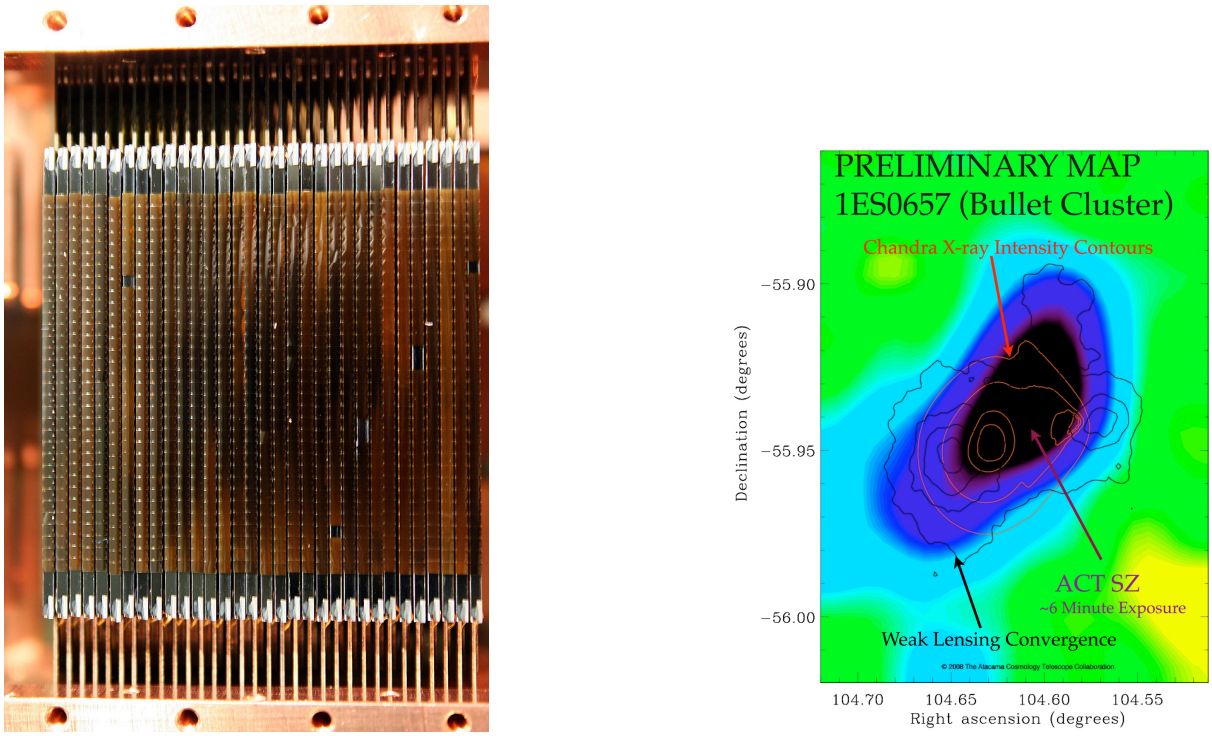

Figure 10. (Left) a photo of the 32×32 array of TES pop-up detectors produced by Princeton and NASA/GSFC. (Right) A 6 minute exposure at 2mm resulting in a Sunyaev-Zel'dovich effect map of the Bullet Cluster [105] proves the power of large arrays.

The MUltiplexed Superconducting TES Array at Ninety Gigahertz (MUSTANG), a collaborative effort between the University of Pennsylvania, NASA/GSFC, NIST/Boulder, NRAO, and Cardiff, is an instrument designed to take advantage of the high angular resolution possible at 3 mm wavelength at the Green Bank Telescope (GBT). The pixels in its 8×8 array subtend around $4''$ each, which, combined with the large scan patterns possible (indeed, necessary) on the GBT, produces large maps with fine detail. This can be seen in Figure 11, where the map width of $\sim 400''$ contains around 3,000 individual beam areas. MUSTANG achieved its first light image on Saturn on September 26, 2006, making it the first operational fully-sampled array at a telescope, and is one of the first to produce astronomical results [106]. Also, while not relevant for satellite or balloon-borne applications, it is worth pointing out that MUSTANG was also the first instrument to collect scientific data with a TES array cooled by a pulse tube cooler.

In August 2005, the NASA/GSFC group kicked off work on a new camera, the Goddard IRAM Superconducting 2 Millimeter Observer (GISMO), a large-field-of-view imager for the 2 mm wavelength band. Optimized for operation at the IRAM 30m telescope [107], it could achieve greater sensitivity to very high redshift sources than cameras operational or proposed at shorter wavelengths [108]. Its 8×16 array of close-packed TES bolometers [109] covers an extent of roughly $2' \times 4'$ by using fast optics providing near-optimal survey speed and source position/flux recovery [110]. The bolometer array is the first fielded array of the backshort-under-grid (BUG)

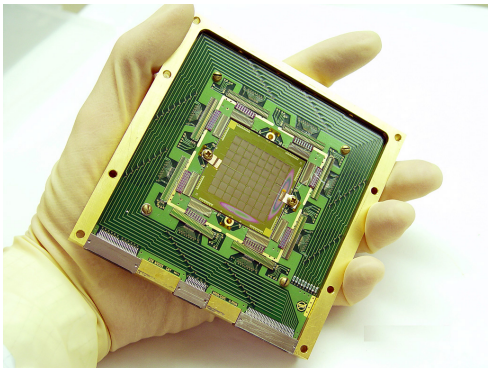

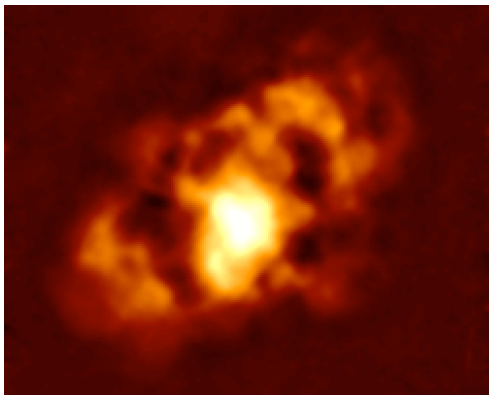

Figure 11. (Left) a photo of the 8×8 array of planar, close-packed TES bolometers fabricated at NASA/GSFC for the U. Penn MUSTANG instrument. (Right) An image at 3mm wavelength of the Crab nebula shows a wealth of structure revealed by the high angular resolution of the GBT.

architecture [111–114], a technology developed to enable and mature versatile, space-qualifiable kilopixel TES arrays with NIST large-format SQUID multiplexers. GISMO achieved first light in November 2007([see Figure 12).

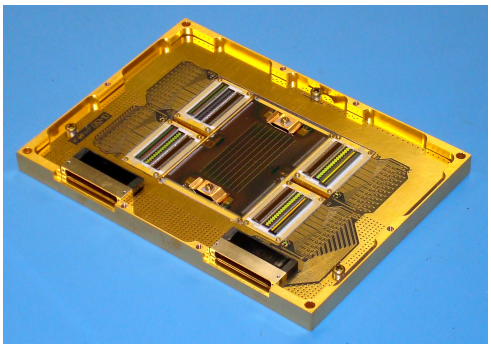

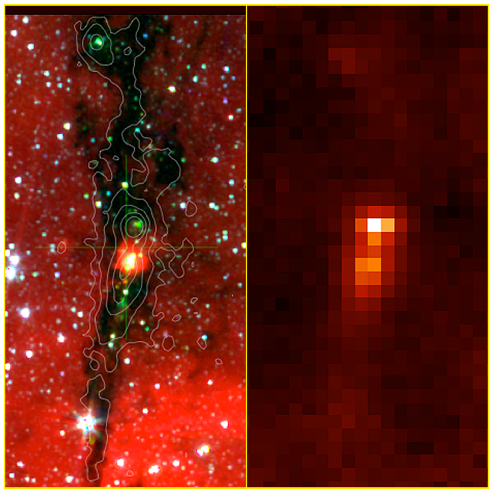

Figure 12. (Left) a photo of the 8×16 array of planar, close-packed TES bolometers fabricated at NASA/GSFC for the GISMO instrument. (Right) An IRAC image with 1.3 mm MAMBO contours shown to the left of the GISMO 2 mm image of the same field: a dense core known as IRDC43.

The South Pole Telescope is another Sunyaev-Zel'dovich-optimized telescope like ACT, but rather larger (10 m as opposed to 6 m) but with fewer detectors (960 as opposed to 3,072). Its first light on a cluster, in April 2007, narrowly beat ACT; however, significant data analysis remains before achieving the theoretical performance [115]. A similar future instrument is CLOVER, again a tri-band system, but aimed at polarimetry of the CMB. CLOVER's compact design [116] is better-suited to detecting B-mode polarization. Its TES bolometer array [117] is made up of individual detectors that are microstrip-coupled to antennas, providing the possibility of packing the array rather differently than would be possible with a monolithic array.

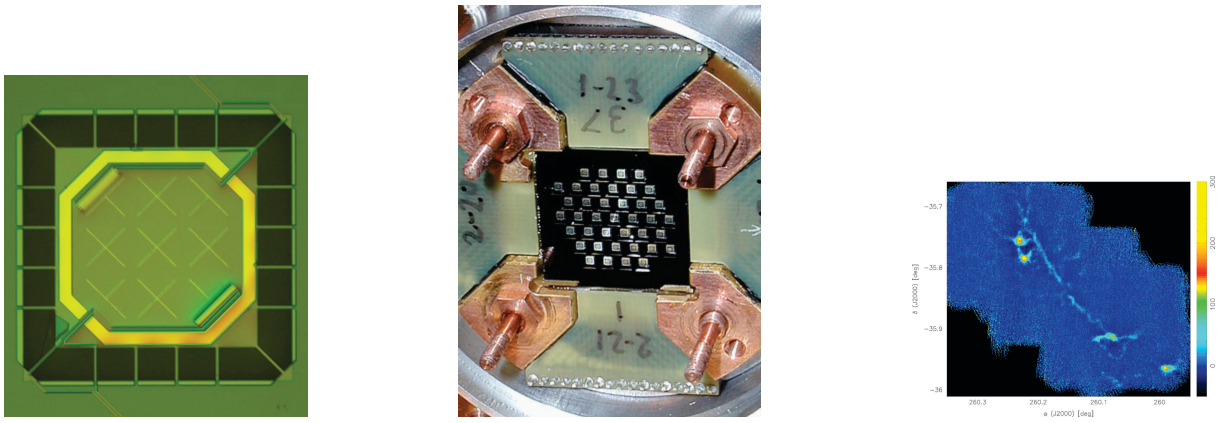

Figure 13. (Left) photos of the 39-element horn-coupled array of TES bolometers fabricated at IPHT/Jena for the MPIfR SABOCA instrument. (Right) A 350 μm image of the NGC6334 star forming region.

A group led by MPIfR at Bonn has developed the SABOCA 350 μm camera, using TES arrays produced at the Institute of Photonic Technology (IPHT) of Jena. Using 39 bolometers coupled to a conical horn array, the instrument saw first light at APEX in May 2008. Photos of its design and an early image are shown in Figure 13. One notable feature of SABOCA relevant to CMB polarimetry is its measured stability (after subtracting correlated sky noise): a noise power spectrum shows no $1/f$ drift down to 0.0025 Hz [118]. Stability on minute timescales makes it possible for even very slow mechanical polarizers to complete a cycle within a bolometer's stability time.

In addition to the above, there are several TES array-based instruments currently in development. I present briefly[5] some sense of what is to come in the next few years, since these may push the technology readiness level (see next sections) better than anything else could before 2010. The most advanced of these is SCUBA-2 [119], which is already at the JCMT and awaiting first light [120]. While it has only single commissioning-grade 32×40 TES arrays in it currently, a set of science-grade arrays is expected in early 2009. The EBEX [121]balloon experiment will fly its $\sim$ 1500 TES bolometers for engineering in 2008 and for science by 2010 [122]. Similarly, SPIDER [123], with its $\sim$ 2600 TES bolometers [124], is scheduled for its first flight in April 2010 [125, 126] Finally, in around 2012, the SAFIRE instrument for SOFIA [127], with its low background kilopixel bolometer arrays [128] for suborbital far-infrared spectroscopy [129], will demonstrate detectors that have passed some of the rigors of design for space flight.

2.6. Technology Readiness Level Assessment (or, where is here anyway?)
This section will cover the Technology Readiness Level (TRL[6]), a minefield of perceptions. Since this assessment is mine and mine alone, it is incumbent upon me to explain in detail why I rate things as I choose to do. A representative definition of the TRL scale is given in Figure 14. The definitions of mid-level TRLs as put forth by John Mankins [130] and as interpreted by this author are provided in Table 1. My scale can be illustrated by the following example: if you

[5] When I say "briefly", I mean that I give almost no details – this is what the cited references are for, if you're curious – and that I cover only a fraction of what is likely to be extant in the coming five years or so. If I tried to be more complete, it would only increase the offense to the ever-shrinking group of experiments that I had omitted, forgotten, was unaware of, or had decided belligerently to ignore.

[6] Note: in speaking, people often refer to the 'TRL level' of a technology. At the risk of arrogant pedantry, I point out that the acronym 'TRL' already contains the word 'level'. Hence, the appropriate phrase is to refer to 'the TRL of a technology.'

intend to produce, starting from scratch, a working large-format TES bolometer array camera for a major project, then your TRLs can be defined as follows: TRL 3 occurs when you have your first working TES devices in your lab cryostat; TRL 4 is reached when a prototype of the flight array is working in the lab; TRL 5 is marked by successfully operating the prototype array on a ground-based telescope and understanding the details of its performance; TRL 6 can be achieved when your completed suborbital instrument flies and/or when your engineering models of the flight array have undergone qualification testing.

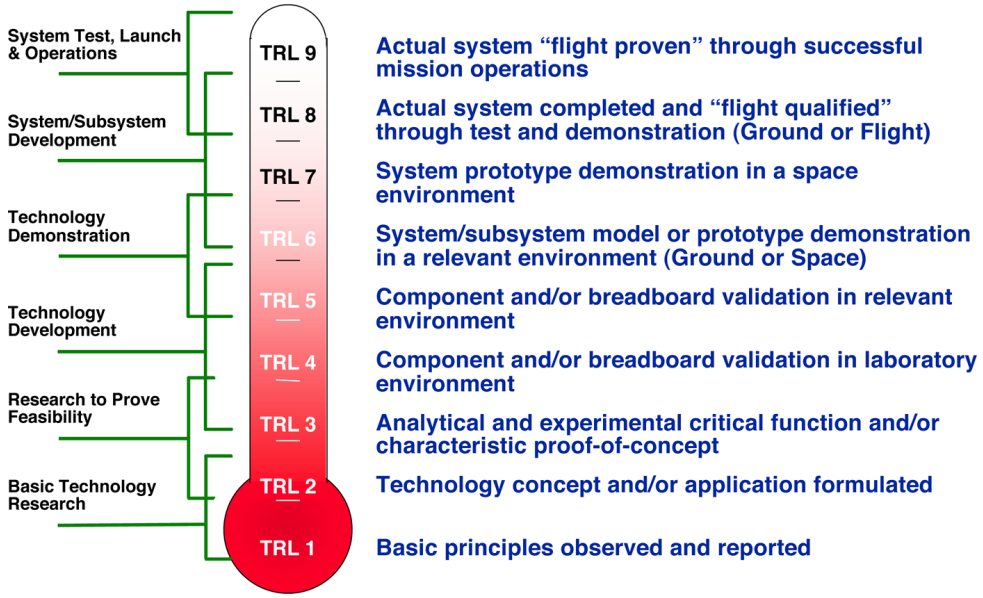

Figure 14. This TRL chart gives the flavor of technology readiness, but interpretation of readiness allows for a latitude of around ±1 when technologies are evaluated by different people. Chart is from NASA's HRST Technology Assessments Technology Readiness Levels [131]

To summarize the positive aspects of what has been achieved to date, I will offer the following off-the-cuff statements that pull together the most important achievements. First of all, several instruments (e.g., APEX-SZ, ACT, MUSTANG, GISMO, SABOCA) exist. That, in the space of less than a decade, the instrumental community has been able to go from barely-proof-of-principle detectors to kilopixel arrays operating near fundamental noise limits is astonishing. People should feel rightly proud of this phenomenal progress. Part of this success concerns the pixel count: SCUBA-2 engendered the 1,280-pixel multiplexer, so an array of around this size is now both state-of-the-art and surprisingly commonplace. Furthermore, this pixel count is probably close to what is needed for a CMB Einstein Inflation Probe. The sensitivity of the detectors listed above is not fabulous (close to an NEP of 10^{-17} W/$\sqrt{\text{Hz}}$ for all of them), because it doesn't need to be. However, this is approaching what is needed for CMB polarimetry from a balloon, and there are efforts ongoing to reach the greater sensitivities needed for CMB polarimetry from space. Finally, one other positive aspect of recent work is that the readouts – varieties of SQUID multiplexers – all seem to function well. Their performance is excellent, and they are generally easy to interface to detector arrays (at least, at the 10^2 pixel level.) In the near-infrared, multiplexers seem to have their own unique quirks that change from generation to generation. My experience with the NIST time domain multiplexers is that they generally continue to become more sophisticated while retaining the same footprint, interfaces, etc. Perhaps future generations of multiplexers will be different, but for the time being, upgrading has been nearly transparent for around five years.

TRL Number & Name	Description	TES Examples
3 Analytical and experimental critical function and/or characteristic proof-of-concept	At this step in the maturation process, active research and development (R&D) is initiated. This must include both analytical studies to set the technology into an appropriate context and laboratory-based studies to physically validate that the analytical predictions are correct. These studies and experiments should constitute "proof-of-concept" validation of the applications/concepts formulated at TRL 2.	Conducting TES noise modeling and experiments. Determining scaling functions of performance parameters. Produce small TES arrays and verify dark performance in the lab.
4 Component and/or breadboard validation in laboratory environment	Following successful "proof-of-concept" work, basic technological elements must be integrated to establish that the "pieces" will work together to achieve concept-enabling levels of performance for a component and/or breadboard. This validation must be devised to support the concept that was formulated earlier, and should also be consistent with the requirements of potential system applications. The validation is relatively "low-fidelity" compared to the eventual system: it could be composed of ad hoc discrete components in a laboratory.	Develop working system for a ground-based instrument and operate it in a laboratory environment. Demonstrate scalability for large-format arrays. Conduct detailed performance tests and evaluate performance under a variety of conditions.
5 Component and/or breadboard validation in relevant environment	At this, the fidelity of the component and/or breadboard being tested has to increase significantly. The basic technological elements must be integrated with reasonably realistic supporting elements so that the total applications (component-level, sub-system level, or system-level) can be tested in a simulated' or somewhat realistic environment. From one- to-several new technologies might be involved in the demonstration.	Deploy a TES instrument to a ground-based platform and produce scientific results. Produce a working integrated large-format detector array system in a laboratory environment.
6 System/subsystem model or prototype demonstration in a relevant environment (ground or space)	A major step in the level of fidelity of the technology demonstration follows the completion of TRL 5. At TRL 6, a representative model or prototype system or system which would go well beyond ad hoc, patch-cord' or discrete component level breadboarding would be tested in a relevant environment. At this level, if the only relevant environment' is the environment of space, then the model/prototype must be demonstrated in space. Of course, the demonstration should be successful to represent a true TRL 6. Not all technologies will undergo a TRL 6 demonstration: at this point the maturation step is driven more by assuring management confidence than by R&D requirements. The demonstration might represent an actual system application, or it might only be similar to the planned application, but using the same technologies. At this level, several-to-many new technologies might be integrated into the demonstration.	Produce an engineering / flight qualification model of a large format TES bolometer array. Successfully qualify mounts, electronics, etc. in appropriate facilities for shock, vibe, EMI, radiation, etc. Operate TES instrument in a fully-remote or autonomous mode. Deploy a TES instrument to a suborbital platform and produce scientific results.

Table 1. Mid-Level Technology Readiness Levels as applied to TES Bolometers

Rosy as the picture above may be, there are significant tasks yet to be accomplished. None of the list I give here is a Herculean task, but often recently it has felt as if the funding available was equivalent to being given a whiskbroom to clean the Augean stables. The first item in priority is the most basic: the maturity of observing with TES bolometers needs to be significantly advanced. When there are facility instruments with TES bolometers, a new community of astronomers will learn to rely on them. When experiments produce reams of data to be analyzed by a science team that has little direct contact with the instruments producing the data, they will learn to extract the best result despite peculiar effects. The wealth of experience with cryogenic semiconducting bolometers (dating back almost 40 years [16]) was a major contributor to the decision to use them on Herschel/SPIRE.

From a theoretical and experimental standpoint, it is essential that the excess noise problem be worked out. That ITFN exists and is calculable is fairly well-established. Other sources of noise such as phase slip or white voltage noise are less well-understood and well-characterized. This should continue to be investigated until some quantifiable prediction of which combination of effects makes up "excess noise".

Another nascent field is that of detector polarimetry. On-chip polarimeters that read out both polarizations, and which might even be able to switch them, are not a mature technology. A ground-based or balloon-borne camera with an appropriate polarimeter using such TES bolometers would be a big step forward.

Finally, there is the issue of space flight qualification. Suborbital experiments such as SAFIRE on SOFIA or the balloon-borne experiments EBEX or SPIDER go a long way to ensuring that a technology is robust enough to be used in a harsh and remote environment, but they do not compare to the rigors of qualification for space flight. This includes designing a detector subsystem for a demanding set of requirements and then conducting a variety of EMI, thermal, and vibration testing. This is expensive work, and probably will not happen without directed CMB polarimetry funding. However, it will eventually be necessary and the sooner it can be done, the better.

Summarizing, my perception is that the TES bolometer array for CMB polarimetry is a technology (really a combination of many technologies) that is close to achieving a TRL of 5. If allowed to use TRL as a continuous scale, I would rank TES bolometer arrays as TRL=4.8. I note that large arrays (kilopixel scale) are just now being fielded, and very little scientifically useful data from TES arrays has been acquired. We have not yet achieved a thorough understanding of the noise properties of real TES bolometers. However, advances are rapid and making headway on all fronts, and perhaps TRL=5.0 will be achieved as the first astronomical data publications emerge from the ACT and SPT collaborations [132, 133].

2.7. TES Detectors in Context (or, what else is here?)

Despite the focus devoted to the transition edge sensor bolometer, it should not be inferred from the above that this is the only detection technology – nor necessarily the best – for a CMB polarization application. It is worth considering the context of other technological approaches, and indeed the overall systems aspects of TES detectors. In considering other technologies, it is important to remember some guiding points about detectors for the CMB. Most importantly, at frequencies near ~ 100 GHz, several competing technologies are close to or below the detector noise equivalent power requirement set by the CMB photon noise in space. Mapping speed is thus improved principally by increasing the number of detectors that can be feasibly deployed in a focal plane array. The detector response time is also important, as is its stability, inasmuch as these constrain the viable scan patterns and polarization modulation schemes that will be used to limit systematics.

The highest maturity direct detector for CMB astrophysics is the semiconducting bolometer, which has been used for decades in the measurement of the spectrum and anisotropy of

the CMB, including in the Nobel-prize-winning space-flight COBE/FIRAS instrument [134]. Semiconducting bolometers are discussed below (Section 3). Their thermal and electrical properties are well-established both experimentally and theoretically (e.g., [37, 135]). The most recent semiconducting bolometers for long wavelength applications have employed advanced absorbers such as the well-known spiderweb bolometers [136, 137]. Large semiconducting arrays exist in ground-based instruments such as SHARC II [138] and BOLOCAM [139], and the balloon-borne BLAST [140]. However, with few exceptions, large scale multiplexing is not possible for such arrays, and hence individual JFET amplifiers must be connected to each pixel, with the large power dissipation and high temperatures inherent from such amplifiers. The low magnitudes of α for semiconducting thermistors result in slower bolometers for a given design than would be the case with a TES thermistor. Also, methods for optical coupling with semiconducting detectors are essentially limited to absorber-coupled (as opposed to antenna-coupled) methods. While none of these are insuperable obstacles, the combination enhances the attractiveness of TES bolometers.

Coherent amplifiers provide another competitive alternative for CMB detection, at least at frequencies up to $\sim$ 100 GHz. The quantum noise of such devices dominates at shorter wavelengths, and in fact extant devices have best performance several times the quantum limit. Thus, there is certainly some cause to consider a mission that has direct detectors in the focal plane as well. As one consideration, the foreground removal requires spanning the wavelength range where synchrotron, free-free, CMB, and dust emission change significantly relative to each other. From the recent summary of Dunkley [141], this will require detectors operating at $\lambda = 1.5$ mm or less, where coherent detectors have a noticeable raw sensitivity disadvantage compared to direct detectors. However, in favor of coherent detectors, it must be admitted that common amplifiers need to be cooled only to $\sim$ 20 K rather than the $\sim$ 100 mK required for bolometers. Mitigating this advantage, however, is the need to provide a much (orders of magnitude) larger cooling power for amplifiers at the higher temperature than would be required for the refrigerators cooling bolometers. Other aspects in favor of coherent detectors are operational simplifications such as wide dynamic range, low nonlinearity, and insensitivity to cosmic rays and microphonics. One disadvantage is the difficulty of producing large format arrays of coherent amplifiers, although this may now have been solved to some degree by the QUIET experiment [142]. It has been noted that coherent amplifiers offer great flexibility in signal processing after amplification, when both amplitude and phase are available, but before power detection, when only amplitude is available. However, TES bolometers can readily be fed by antennas through microstrip (e.g., [4–8]), permitting many of the same capabilities. Overall, given that covering all the frequency bands necessary for CMB polarization measurement with a sufficient number of pixels at sufficient sensitivity is of paramount importance, it seems that coherent detectors require further development to enable a CMB polarization space mission.

On the topic of further development, it is worthwhile to note that bolometers as a whole have made great strides in sensitivity over a very long history (Figure 15). Even within the limited realm of NASA-relevant work, there are non-CMB applications for bolometers (the far-infrared has been noted above in several instances, and the closely-related x-ray microcalorimeter detectors are fundamentally little different). As a result, per-pixel sensitivity has now achieved the sensitivity requirement of CMB (Figure 15) applications in space. Further strides in overall mapping speed are now being made by the investment in large format bolometer array development. This is where CMB-targeted technology maturation is needed.

To summarize some of the advantages of TES bolometers as compared to other relevant technologies, there are relatively few points. Their sensitivity permits background-limited operation at all wavelengths needed for CMB polarization measurements. Large format arrays have been demonstrated using SQUID multiplexers, which yield excellent mapping speed. The accelerated response time permits a range of viable scan patterns and polarization modulation

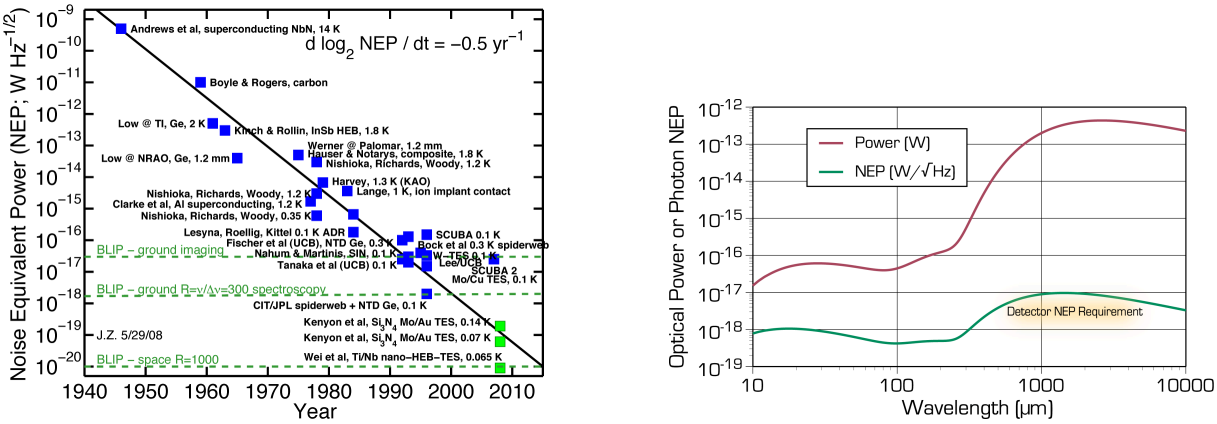

Figure 15. (Left) The NEP of bolometers has improved by a factor of two every two years for more than half a century (figure courtesy of Jonas Zmuidzinas). (Right) The natural sky backgrounds in space require detectors of a sensitivity that is now easily reached by bolometers. Larger format arrays continue to improve the effective mapping speed of fielded instruments where background-limited sensitivity has been achieved.

timescales. Some improvement may be realized in dynamic range and stability. Multiple groups now have experience in fabricating, testing, and fielding TES bolometer arrays, and so their heritage is substantial enough that development for space applications is appropriate.

2.8. TES Development Plan (or, From Here to Launch!)

This highly-speculative section approaches the task of how to prepare and mature the TES component technology for the cosmic microwave background polarimetry. Thus far, very little has had any focus on this one mission, instead being an overview of the field as it related to superconducting bolometers at long wavelengths in general. Measurements of CMB polarization promise to allow us to distinguish among models of the first instants of our universe. Advancing detector array technology is a stepping-stone to the goal of arrays of polarization sensitive detectors required for missions such as the Einstein Inflation Probe (when used with specific coupling and modulation structures under development elsewhere). Further in the future, even larger arrays are a requirement for the efficient use of large cryogenic telescopes in space such as SAFIR [143] and SPIRIT [144].

In my consideration, I take it as a governing assumption that TES bolometer arrays must be perceived to be mature in order for them to form the basis of a CMB polarization Einstein Probe mission. While Probe-class missions ($\sim$ \$600 M cost class) could, in principle, provide their own technology development initiatives, it seems equally likely that an insufficiently mature technology could, conversely, hinder the initiation of funding for a Probe. Hence, the perception of TRL=6 may be required in order to bring about a successful Einstein Inflation Probe. How can this be achieved?

The most effective way to rapidly increase the perceived maturity of TES bolometers will be to deploy larger, higher performance detector arrays in existing instruments or on existing telescopes. These will then need to be used regularly for major experiments or facility instruments. Through scientific use, we discover the interactions of the detectors with other elements of the experiments, and techniques for their mitigation. The technologies to build and read out multi-kilopixel arrays are just now well-established enough that there are multiple possible approaches and facilities for their production. Having a wealth of astronomical

data and – more importantly – understanding of TES bolometers by astronomers[7] is critical. Facility instruments on ground-based telescopes both (1) allow a bigger 'credibility pool' for the technology and (2) bring more minds to bear on teasing out effects in the data.

A second, and I would hope simultaneous, path is to pursue the theoretical explanations for excess noise. This issue does not appear to be firmly settled, and a combination of theorists (to quantify predictions, estimate observables, and explain how to distinguish between the original causes) and experimentalists (whose job it is to provide high quality – and by that I mean both accurate and precise – data in order to disagree robustly with as many theories as possible) should continue this work. Before proposing a major space mission, it is certainly a good idea and might effectively by required, that we know how to predict the performance of a given TES bolometer correctly *ab initio*.

As a third item – in sequence rather than priority – is that it is imperative a collaboration successfully conducts a suborbital CMB investigation using a TES-based instrument. This is not news to anyone, but it's worth pointing out that while this is the venue that might provide TRL=6 for TES bolometers, modification of the array design approach that is flown on a balloon reduces this to the extent that there is an insufficiently rich body of knowledge at the TRL=1 to 5 level. Thoroughly prosecuting the above two elements will result in a more concrete estimate of the technology readiness – and will, truly, mature the technology.

2.9. Acknowledgements
In the writing of this article, I found help and guidance from many publications and people, the latter class containing: William Duncan, Lyman Page, Giorgio Siringo, Harvey Moseley, Adrian Lee, Jamie Bock, and Nikhil Jethava. I trust Kent Irwin and Gene Hilton to such a degree that I pretty much lifted equations from their paper to write my TES theory section. This research has made use of NASA's Astrophysics Data System Bibliographic Services.

3. Semiconductor Bolometers for Cosmic Microwave Background Polarization Studies

by Harvey Moseley

3.1. Abstract
I will review the state of development of semiconducting bolometers, their prospects for future Cosmic Microwave Background (CMB) polarization experiments, and the effort required for their successful deployment.

3.2. Introduction
Bolometers are thermal detectors which are comprised of a radiation absorber, a thermometer which senses the temperature rise in the detector due to the absorption of radiation, and a conducting link through which the detector is held in thermal contact with a heat sink (Figure 16). Benford 2.2 has reviewed the history of their development in theory and practice.

Semiconducting bolometers have been the mainstay of CMB experiments which use direct detectors (COBE/FIRAS, COBE DIRBE, MSAM,IRTS, Boomerang, MAXIMA, e.g)[145–152]. The Ge or Si-based impurity conduction thermometers have predictable temperature coefficients of resistance, noise, limited by thermodynamic fluctuations and Johnson noise, which agrees well with Mather's [37] theory, and can be designed and optimized for background limited

[7] By "astronomers", I mean here those people derisively referred to as "God damn user astronomers" by a notable Caltech professor, by which he meant that class of astronomers that can acquire great skill at observing using an instrument about which they understand next to nothing.

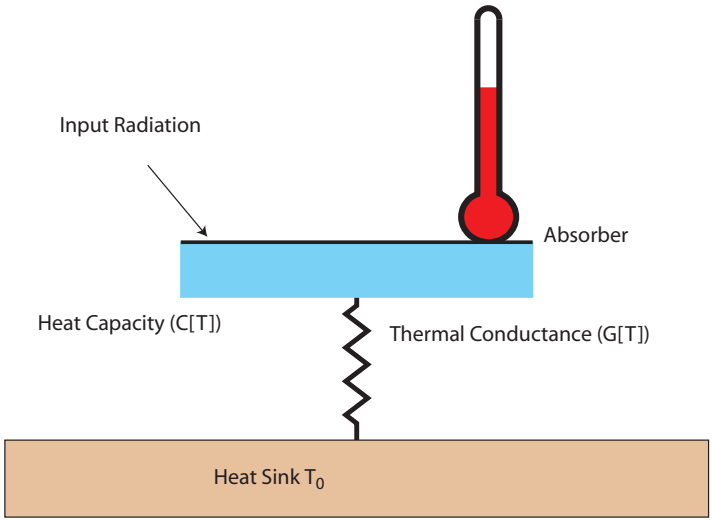

Figure 16. The basic components of a bolometer are shown. The response and minimum noise of such a system can be determined from thermodynamic quantities [37]

performance over a wide range of conditions covering proposed CMB experiments. Typically these thermometers are thermally connected to an absorbing element, which can be separately optimized, commonly using a resistive metallic film to absorb the incident radiation.

With a change of optical instrumentation and absorber structures, these detectors have been used for for CMB polarization measurements (Boomerang,Maxipol, e.g). In this paper, I will discuss the present state of semiconducting bolometers, their suitability for CMB studies, and consider their future prospects

3.3. Development

While Ge:Ga bolometers were introduced into infrared astronomy by Low [16], it was in the early 1980s that full promise of these devices was realized and developed. Mather [37] developed a theory which accurately describes the noise and response of such a detector, and provided clear insight into the scaling of the performance of the detector with temperature, conductance, heat capacity, and thermometer sensitivity. In his 1984 paper [135], he describes the optimization of such a detector. Following his procedure, we assume that for a given application, the radiant power is given, and there is a minimum detector heat capacity required to provide absorption and thermometry in the detector. Taking the absorbed power, signal modulation frequency range, detector heat capacity, and the thermal sensitivity

$$\alpha = \frac{dLog(R)}{dLog(T)} \tag{14}$$

of the detector as givens, the optimization of the detector consists of simultaneously adjusting the thermal conductance between the detector and its heat sink and the amount of bias power

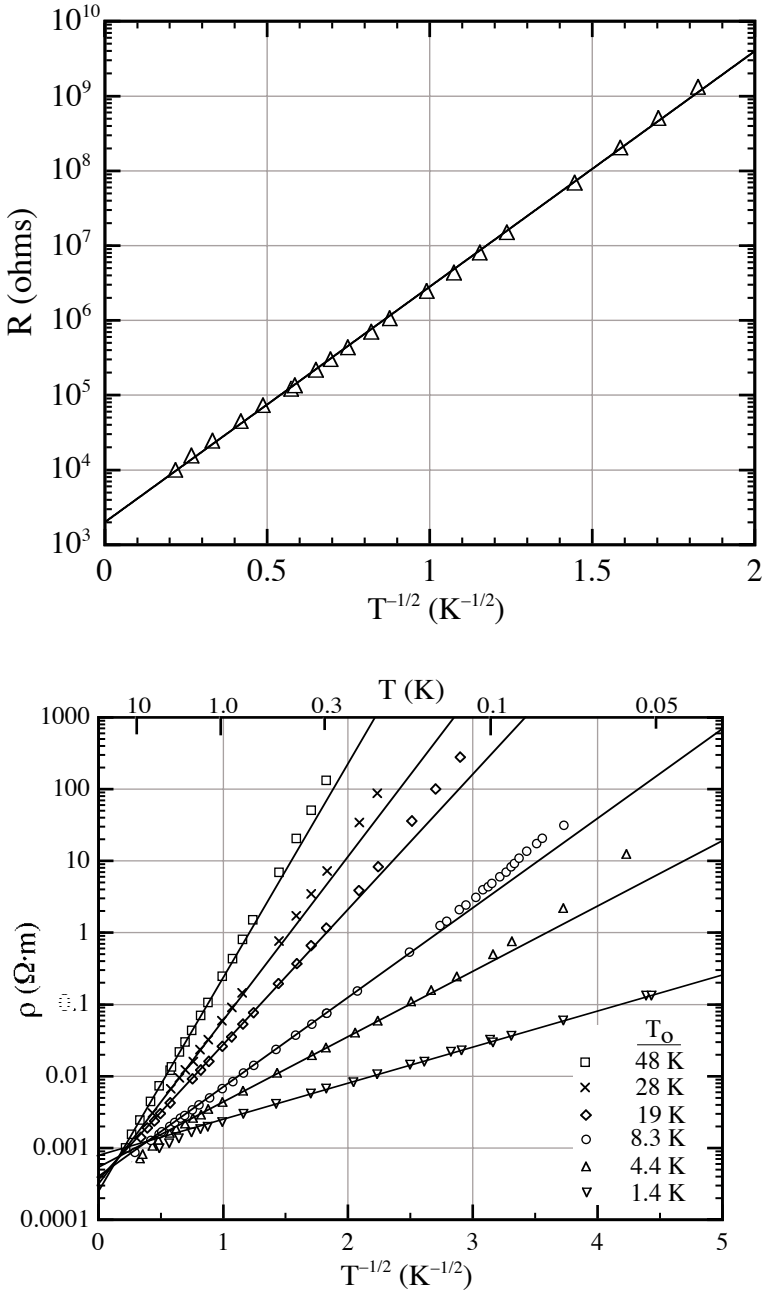

Figure 17. (Left) The resistance of impurity conduction thermometers in Si is well described over five orders of magnitude in resistance by the variable range hopping model. (Right) This theory accurately models impurity conduction of Si in the low temperature regime over a wide range of resistances and impurity concentrations [51]

dissipated in the detector to minimize system noise. The result of this optimization, shown as a function of α is seen in figure 18. Several general results arise from this simple analysis:

(i) For a thermal conductance $G \propto T^3$, the detector Noise Equivalent power (NEP) scales at $T^{\frac{5}{2}}$

(ii) For a given background power and wavelength, the detector noise can be designed to be below the background noise by lowering its operating temperature sufficiently

(iii) Higher values of the thermometer sensitivity, α, results in more response bandwidth.

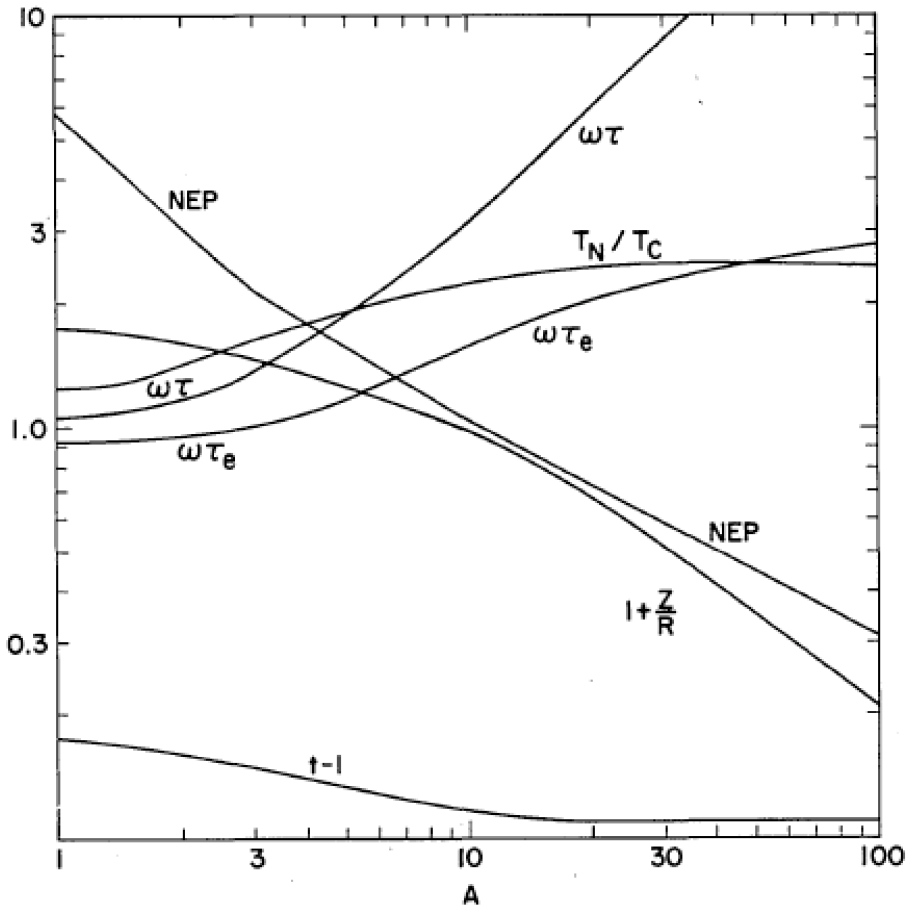

Figure 18. Using his thermodynamic model for bolometer performance in the linear regime, Mather [135] shows the optimal performance and detector operating conditions as a function of thermometer sensitivity α.

At the time of this work, semiconductor processing techniques were, for the first time, being applied to the development of bolometers, both in Si and Ge [26, 153]. The application of ion implanted contacts eliminated these elements as a source of noise. The advent of micromachining techniques permitted the development of very low heat capacity detectors, and the demonstration of the thermometers at $T \sim 0.1\ K$ brought the sensitivity required for a wide range of experiments, including CMB studies, within the available design space. The reproducibility of the devices arising from the improved fabrication techniques made large (~ 100 elements) arrays practical.

3.4. Semiconductor Thermometers

The conduction mechanism in these Si and Ge impurity conduction bolometers is variable range hopping, seen in semiconductors doped near the metal-insulator transition. While the detailed physics of this transport process is complicated, experimenters have explored the conduction and noise properties of these thermometers as a function of impurity concentration, temperature, and current density [154, 155]. These measurements provide the basis for the design and optimization of bolometers for a wide range of experimental conditions The performance of Si and Ge thermometers are similar, with Ge having an advantage over Si at low temperature based on the ratio of the thermometer sensitivity to its heat capacity. But for the purpose of producing detectors for CMB polarization, which is a high background power application, the thermometer decision can be made on the basis of ease of fabrication. McCammon [51] has written a comprehensive review of the properties of semiconducting thermometers, and discusses the detector design process.

3.5. Amplifiers and Readout

The primary shortcoming of these semiconductor bolometers has been the lack of suitable amplifiers and multiplexers which can be integrated with them at the focal plane temperature. The noise of the detectors is typically double the Johnson noise of the thermometer, so amplifiers with noise temperatures lower than the physical temperature of the detector are required. The most convenient high performance amplifiers are JFETs, which require thermal ionization of carriers to function, and thus typically operate in the 70 to 150 K range. At this temperature, they can provide equivalent noise temperatures $\sim 0.1\,\mathrm{K}$, adequate for most present bolometer applications. Typically, detectors have been operated with a single JFET per detector, which has required significant cryogenic/electrical engineering to produce low noise, low power dissipation system. Modules in which the JFETs are suspended on thin Si_3N_4 membranes have been developed for the SPIRE instrument on ESA's Herschel. Each module, with 16 JFETs, dissipates 5 mW of power, or about $300\,\mu$W per channel, typical of other designs [156]. The XRS instrument on Astro-E2 used a two stage isolation system for the FETs, so that much of the power could be dumped into the intermediate heat sink at 16 K. This resulted in a 32 channel system in which a total of less than $100\,\mu$W was sunk at the 2 K heat sink [157]. While both these systems were successfully engineered, systems with an order of magnitude more pixels than existing devices will present a major technical challenge.

Billot et al. [158] have developed a semiconductor-based detector array which is being used in the PACS instrument on Herschel. This device uses MOSFET switches for multiplexing, and MOSFET amplifiers operating at the detector temperature. While this is conceptually appealing, the relatively high noise of MOSFETs at low frequencies requires very high resistance detectors to avoid amplifier noise limitations. This results in long RC time constants, which significantly limit the response bandwidth of the detector. The $\frac{1}{f}$ noise of the MOSFET can be corrected by sampling a stability reference in the course of the readout. The greatest practical limitation of this design is that given the level of amplifier noise, only about 16 channels can be multiplexed using a single amplifier output. This has significant power and complexity implications for large format arrays, but this simple and compact design has advantages for some applications

3.6. Present State of Development

Semiconductor bolometers are well developed for space flight missions. They have been flown and operated successfully on many missions, including COBE, IRTS, and Astro-E2, and large focal plane arrays will soon be launched on Planck and Herschel. This history suggests that the semiconducting detectors have a high technical readiness level, say TRL 9. However, since the detailed detector designs which we would fly on a CMB polarization mission could

differ significantly from those flown on earlier missions, significant qualification work is must be anticipated to demonstrate flight readiness. To be more specific, the technology is well qualified, but the specific designs must be developed and tested.

3.7. Prospects
Semiconducting bolometers can provide adequate sensitivity for strongly background limited operation in future CMB missions. They are technically well developed, have predictable performance, and are easy to adapt to a wide variety of optical systems. However, significant work is required to integrate these detectors with planar mm-wave detector circuits being developed for CMB polarization missions. Despite their general maturity, significant effort would be required to adapt these detectors to the present generations of instruments, but it is likely that this could be successfully accomplished. The major factor limiting the utility of these detectors for future missions remains the lack of availability of low noise amplifiers which can be closely integrated with the detectors. This results in a complex system design and integration process. The mechanical and thermal engineering challenge of interfacing between hundreds of 120 K JFET amplifiers and detectors below 0.1 K is one that can be attempted, but with thousands of detectors, this daunting task is a major risk to mission development. However, if high performance alternatives did not exist, these detectors could be developed to enable CMB polarization science.

3.8. Acknowledgments
I thank Dan McCammon, Kent Irwin, Dominic Benford, and David Chuss for help in preparing this review.

4. Superconducting Microresonator Detectors

by Jonas Zmuidzinas

4.1. Technical Description
4.1.1. Basic Physics The basic concept of operation is described in a number of publications [159–164] and is illustrated in Fig. 19. Photons are absorbed in a superconducting film, which causes Cooper electron pairs to break. The binding energy of Cooper pairs is proportional to the critical temperature, $2\Delta \approx 3.5 k_B T_c$, which corresponds to a minimum photon frequency $\nu = 2\Delta/h \approx 90$ GHz for aluminum ($T_c = 1.2$ K). A perturbation δP of the absorbed mm-wave power thereby produces a perturbation $\delta Z_s = \delta R_s + j\delta X_s$ of the complex microwave surface impedance of the film. Both the real and imaginary parts of the impedance are affected in this process: Cooper pair breaking causes the surface reactance to increase (this is the "kinetic inductance" effect), and meanwhile the single electrons (or "quasiparticles") that are produced are capable of scattering, and are therefore dissipative, and are responsible for an increase in the surface resistance. Both of these effects can be sensed by incorporating the superconducting film into a resonant circuit and measuring the resulting changes in the resonance frequency and quality factor, as shown in Fig. 19.

The readout of the resonator can be explained more precisely by considering the trajectory of the complex microwave transmission $S_{21}(\omega)$ in the complex plane as the angular (microwave) frequency ω is varied. The linewidth of the resonance is $\Delta\omega_r = \omega_r/Q_r$, where the resonator's quality factor is determined by coupling and internal losses according to the usual formula, $Q_r^{-1} = Q_c^{-1} + Q_i^{-1}$. Away from resonance, the transmission is essentially unity $|S_{21}| = 1$, and near resonance describes a circle with the resonance frequency being the point of closest approach to the origin, as shown in Fig. 19. If the readout generator's frequency ω_g is fixed,

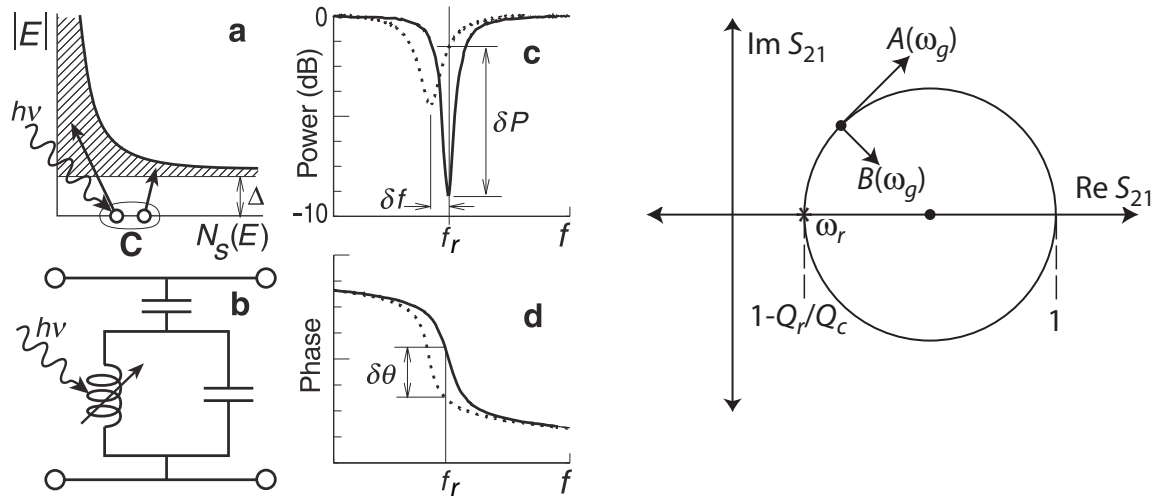

Figure 19. Left: Principle of operation of superconducting microresonator detectors, following [159]. The absorbed photon energy breaks Cooper electron pairs in a thin superconducting film (a) which is part of a lithographed microresonator circuit (b). The breaking of Cooper pairs causes a change in the surface reactance and resistance of the film, leading to a shift in the resonance frequency f_r and a reduction of the resonator's quality factor Q_r (c), which can be sensed by measuring the phase (d) and amplitude (c) of the microwave output signal. **Right**: This figure illustrates the trajectory of the resonator's transmission $S_{21}(\omega)$ as a function of angular frequency ω in the complex plane. The transmission is unity ($S_{21} = 1$) at frequencies away from resonance. Starting at a frequency below resonance, S_{21} traces out the circle in a clockwise direction as the frequency is increased, crossing the real axis at the resonance frequency ω_r indicated by the star, and corresponding to a transmission $S_{21}(\omega_r) = 1 - Q_r/Q_c$ as indicated, where Q_c is the coupling-limited quality factor. The adiabatic response coefficients for changes in the resonator frequency $A(\omega_g)$ and dissipation $B(\omega_g)$ are shown for the case that the generator frequency ω_g is tuned above the resonance. These coefficients are tangent to and perpendicular to the resonance circle, respectively.

and a change in optical power δP is introduced, the resulting change in the surface reactance δX_s will cause a perturbation in the complex transmission δS_{21} that is tangent to the resonance circle; meanwhile, δR_s causes δS_{21} to move in a perpendicular direction. The overall response is the vector sum of these two components. Therefore, by using readout electronics that are capable of real-time vector measurements of S_{21}, one can simultaneously measure and separate these two effects. However, the perturbation in the reactance is a stronger effect: the ratio is $\delta R_s/\delta X_s \equiv \tan\psi \approx 0.3$ [164–166]; this ratio also describes the relative strengths of the transmission perturbations δS_{21} for the tangent and perpendicular directions. This is of practical importance: the factor of $\sim 3-4$ lower responsivity for the dissipation readout places more stringent demands on the noise performance of the cryogenic microwave amplifier that follows the resonator (see section 4.1.4).

4.1.2. A millimeter-wave implementation A practical implementation of this concept for mm-wave detection is shown in Fig. 20, using a quarter-wavelength transmission-line resonator rather than a lumped-element circuit. A coplanar waveguide (CPW) transmission line allows the

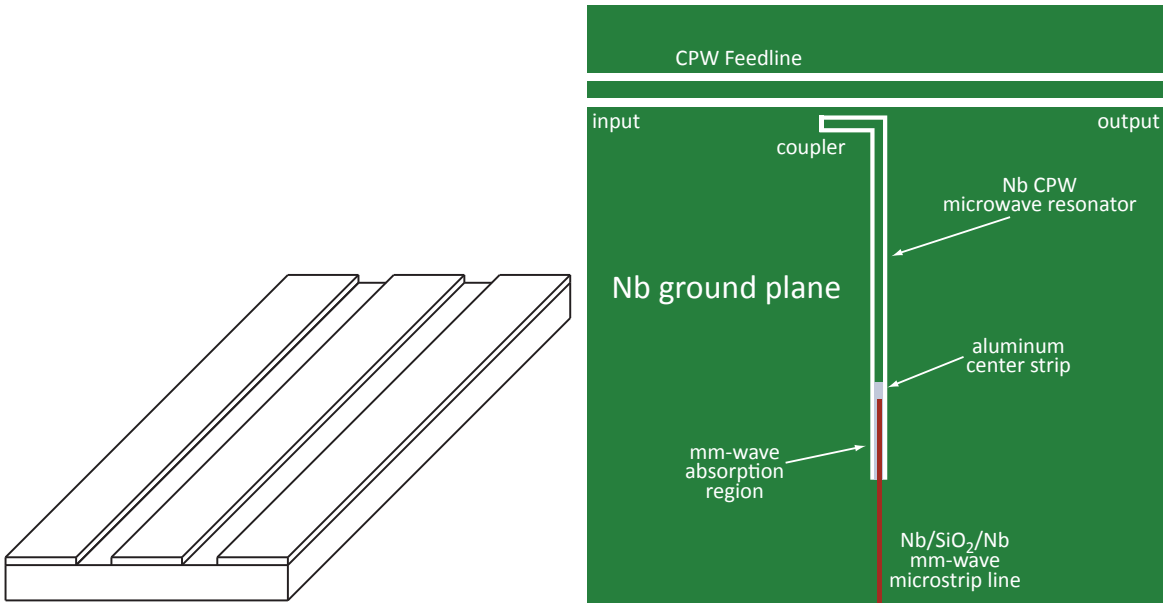

Figure 20. Left: A coplanar waveguide (CPW) transmission line is fabricated by etching two parallel slots in a metal film, which defines a center conductor and two ground planes. **Right**: A typical microstrip-coupled mm-wave detector made using a hybrid niobium/aluminum (Nb/Al) CPW quarter-wave resonator. The resonator is short-circuited at the bottom, where the mm-wave radiation is absorbed, and is open-circuited at the top, where the resonator is coupled to the feedline. The microwave readout signal propagates along the CPW feedline at the top, fed from the signal generator on the left and coupled to the cryogenic low-noise amplifier on the right. The readout signal excites the resonator via the coupler section; the length of the coupler and its separation from the feedline dictate the value of the coupling quality factor Q_c. At the short-circuit end, a strip of aluminum is used for the CPW resonator center strip in place of niobium, because the superconducting gap energy of aluminum allows it to absorb mm-wave radiation with frequencies above 90 GHz; the corresponding gap frequency of niobium is 700 GHz. The mm-wave radiation is coupled to the aluminum strip using a low-loss $Nb/SiO_2/Nb$ microstrip (parallel-plate) transmission line, as shown, and is absorbed over the ~ 1 mm length of the aluminum strip. The typical dimensions are $6\,\mu$m for the CPW center strip width, $2\,\mu$m for the CPW slot, and ~ 5 mm for the resonator length, giving a resonance frequency around 6 GHz.

resonator to be made without the use of deposited dielectric films (which are amorphous and generally lossy [167]), thereby allowing extremely high quality factors ($Q_r \sim 10^6$) to be achieved. The use of an aluminum section near the shorted end of the resonator allows absorption of mm-wave radiation at freuencies above 90 GHz (a lower T_c material would be needed for frequencies below 90 GHz). The mm-wave radiation is brought to the resonator using a low-loss $Nb/SiO_2/Nb$ microstrip line which runs across the aluminum center strip of the CPW resonator, at which point it becomes a $Nb/SiO_2/Al$ microstrip, causing mm-wave dissipation and pair-breaking in the Al strip.

The use of microstrip coupling allows this type of detector to be used with a variety of feeds, including narrow-beam phased-array planar antennas [168–174] with either single or dual-polarization response, broad-beam planar antennas [175–180], and the more traditional horn-waveguide-probe coupling approaches [181–185].

Other coupling techniques are possible, and indeed necessary at frequencies above 700 GHz where niobium microstrip lines become exceedingly lossy. Coupling of far-infrared radiation into an aluminum CPW resonator directly attached to a twin-slot antenna has been demonstrated [186]. Another possibility is to design the inductive portion of the resonator to simultaneously be a good far-infrared absorber. This approach has also been demonstrated [187, 188] and leads to two-dimensional pixel arrays similar to absorber-coupled transition-edge sensor (TES) bolometer arrays. Other approaches for far-infrared microresonator detectors are also being actively pursued (E. Wollack, priv. comm.).

4.1.3. Frequency multiplexing Because the resonators have high quality factors ($Q_r = 10^4 - 10^6$), a large number of resonators may be multiplexed in the frequency domain and read out with a single cryogenic microwave amplifier, as shown in Fig. 21. In this scheme, the resonators are coupled to a common feedline and therefore the detector chip is fully multiplexed, as opposed to TES designs which require multi-lead superconducting connections between the detector and SQUID multiplexer for each pixel (this is true for all types of SQUID multiplexing - time domain as well as MHz/GHz frequency-domain). The room-temperature electronics then has the job of generating a set of excitation frequencies - one per resonator - and then measuring the amplitudes and phases of these signals after they have been sent into the cryostat, transmitted past the resonator array, and amplified by the cryogenic amplifier and any additional room-temperature amplifiers. Fortunately, this task has become quite feasible using modern digital signal processing techniques.

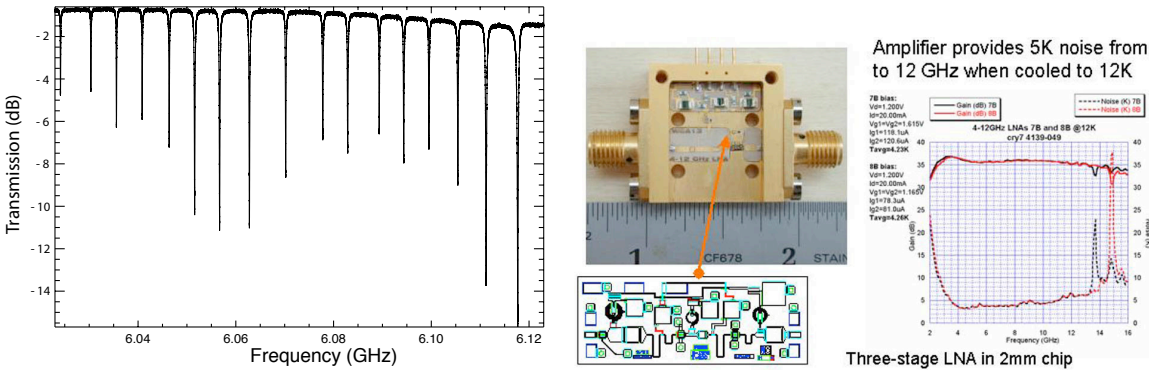

Figure 21. Left: an example of an array of resonators coupled to a single feedline. The depths of the resonances depend on the coupler design and the value of the coupling quality factor Q_c (credit: B. Mazin). **Right**: A single wide-band cryogenic HEMT amplifier (credit: S. Weinreb). can be used to simultaneously measure a large number ($\sim 10^3$) of resonators.

4.1.4. Sensitivity

Fundamental Limits: The fundamental sensitivity limit for this type of detector is set by the random generation of quasiparticles by pair-breaking thermal phonons, and their subsequent recombination. However, this mechanism is exponentially suppressed at low temperatures by the Boltzmann factor $\exp(-\Delta/k_BT)$ due to the superconducting energy gap, and therefore in practice the sensitivity is determined by other factors. Ideally, the sensitivity would be set by photon arrival statistics - the BLIP limit. One interesting subtlety is whether the BLIP limit for these detectors corresponds to a "photodiode" or "photoconductor" device – the latter being

less sensitive by a factor of $\sqrt{2}$ due to the additional noise introduced by the random carrier lifetimes (recombination noise). The answer is "both"! For photon energies just above the gap, $h\nu = 2\Delta + \delta E$, only a single Cooper pair is broken, and an equal amount of noise is generated in quasiparticle recombination. Far above the gap, $h\nu >> 2\Delta$, a large number of quasiparticles are produced, and each quasiparticle recombines randomly, so the recombination noise is averaged down to an insignificant level and "photodiode" performance is obtained.

Conditions for Achieving BLIP Operation: Achieving the BLIP limit requires that the amplifier noise contribution be brought below the photon noise. This requires optimizing the responsivity of the device, which in practice amounts to choosing the correct value of the coupling quality factor Q_c. For low photon backgrounds, the number of photo-produced quasiparticles will be small, and so the resonator's internal dissipation Q_i^{-1} due to the quasiparticles will also be small; conversely, for large backgrounds the dissipation will be larger, and the quality factor will be lower. The coupling strength which maximizes the responsivity is given by $Q_c = Q_i$ [164]. This design optimization is analogous to choosing the desired value of thermal conductance G for a bolometer given the expected optical loading. The second key issue for achieving BLIP is the noise performance of the cryogenic amplifier that is required for an optimized detetector ($Q_c = Q_i$). This question has been studied in some detail theoretically; the answer [164] depends on a number of factors including the gap frequency, the photon frequency, the background loading, the quasiparticle lifetime, the maximum microwave readout power, and crucially, on whether one is using frequency or dissipation readout (see the discussion in section 4.1.1). Calculations [164] indicate that readily achievable amplifier noise temperatures in the range $T_n = 10 - 20$ K would allow BLIP operation using frequency readout, whereas much better performance ($T_n = 1 - 2$ K) is needed for dissipation readout. Because the amplifier contribution to the noise equivalent power (NEP) scales as $\sqrt{T_n}$, the use of a typical HEMT amplifier (see Fig. 21) with $T_n = 5$ K for dissipation readout will result in an NEP value that is roughly twice the BLIP limit. Finally, although the detailed physics of quasiparticle recombination is not fully understood yet [189], the measured lifetimes are sufficiently long and do not impose a serious limitation on CMB observations.

Excess Frequency Noise: Although amplifier noise considerations lead one to focus on using frequency readout, it turns out that CPW microresonators suffer from excess frequency noise. This excess noise prevents the detectors from achieving BLIP performance by a factor of around $5 - 6$ [164] when using frequency readout. The excess noise problem was appreciated early on [159] and stimulated efforts to determine the source of the noise and its general properties. The excess frequency noise rises at low frequencies but has a relatively shallow spectrum, $\sim 1/f^{0.5}$ (see Fig. 22), which implies that the NEP varies very slowly, as $1/f^{0.25}$. The early evidence indicated that the noise did not originate in the superconducting films but rather in the substrate or its surface [162]. Therefore, by using very thin superconducting aluminum films ($t \sim 40$ nm), the frequency responsivity of the device was increased dramatically, and allowed the NEP at 1 Hz to be reduced from the $\sim 10^{-15}\,\mathrm{W}/\sqrt{\mathrm{Hz}}$ level in 2003 to $\sim 10^{-17}\,\mathrm{W}/\sqrt{\mathrm{Hz}}$ in 2005.

Pushing Toward BLIP Performance: Further work [165] showed that the noise really affects just the resonator frequency; no excess noise was seen in the dissipation signal above the level of the amplifier noise (see Fig. 22). This of course opens up the possibility of using the dissipation readout with very high-Q resonators in order to achieve very low NEP values, and this idea has been actively pursued by the SRON group [191, 192]. Their lowest achieved NEP to date is $7 \times 10^{-19}\,\mathrm{W}/\sqrt{\mathrm{Hz}}$ and is steadily decreasing as the quality of the devices and measurement setup are improved. Although this NEP value is actually better than required for broadband CMB measurements, the NEP will degrade as optical loading is applied because the resonator

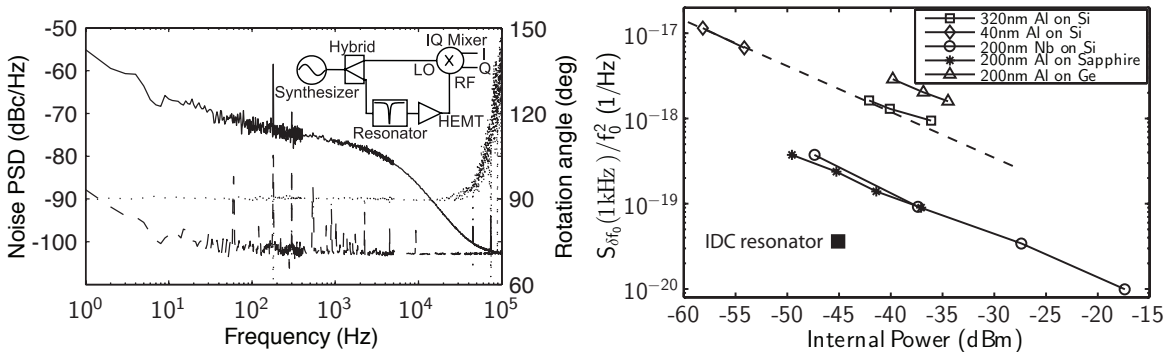

Figure 22. Left: An example [165] of the measured noise power spectra for frequency readout (solid line) and dissipation readout (dashed line). The dotted line indicates the rotation angle between the direction of minimum noise and the tangent to the resonance circle; a value of 90 degrees indicates that the noise is essentially entirely due to frequency noise. Significant excess frequency noise is seen, whereas the noise floor for the dissipation readout is set by the cryogenic HEMT amplifier. The quality of the noise spectra below 10 Hz are limited by insufficient integration time but may be showing $1/f$ amplifier fluctuations; if necessary, such fluctuations can be removed using a variety of techniques, or possibly by using SiGe bipolar amplifiers with low $1/f$ noise. The frequency noise shows a $1/f^{0.5}$ slope in the 10 Hz to 10 kHz range; the corresponding NEP varies as $1/f^{0.25}$. The inset shows the usual homodyne readout scheme. **Right**: This plot [165] shows the typical range of fractional frequency noise measured for CPW resonators. The frequency noise exhibits a $P^{-1/2}$ dependence on the microwave readout power. The square point represents very recent results using a new resonator design [190] that incorporates an interdigitated capacitor (IDC).

quality factor will be reduced. The conclusion is that even for CMB measurements from space, microresonator-based detectors used in dissipation readout mode can already achieve sensitivities within a factor of 2 or so from BLIP.

One approach to push closer towards the BLIP limit is to use dissipation readout with a lower-noise amplifier. Good progress is being made in this direction through the work by Weinreb and colleagues [193, 194] on cryogenic SiGe bipolar amplifiers; noise temperatures of order 2 K have been achieved at frequencies below 2 GHz. Note also that these amplifiers may be expected to have very low $1/f$ gain noise, which should reduce the need to apply other techniques for measuring and compensating the amplifier's gain fluctuations.

Another route is to reduce the resonator frequency noise. It has recently been demonstrated [164, 195, 196] that the noise almost certainly originates primarily from a layer on the surface of the device. This surface layer contains two-level defects such as are commonly found in amorphous dielectric materials, and the fluctuation of these two-level systems (TLS) introduces noise in the resonator due to coupling of the TLS electric dipole moments to the resonator's electric field. A semi-empirical, quantitative theory of this noise mechanism has been developed [196] in which the TLS noise contribution scales as the cube of the electric field, $|E|^3$, and therefore those TLS located near the open-circuit end of the resonator are the most harmful. This insight has been used to develop a modified resonator geometry, in which the high-field "capacitive" portion of the CPW resonator is replaced by an interdigitated capacitor (IDC) structure with $10 - 20$ μm electrode spacing, as compared to the 2 μm spacing used for the CPW line. Recent measurements [190] show that this new IDC design has dramatically lower noise (see Fig. 22), currently by about a factor of 10 in terms of the frequency noise power

spectrum, corresponding to a factor of $\sqrt{10}$ in NEP. These results confirm essential aspects of the noise model and again show that the noise really is not related to the superconductor. Further significant noise reductions may be expected in the future as the insights offered by the new noise model are more fully exploited.

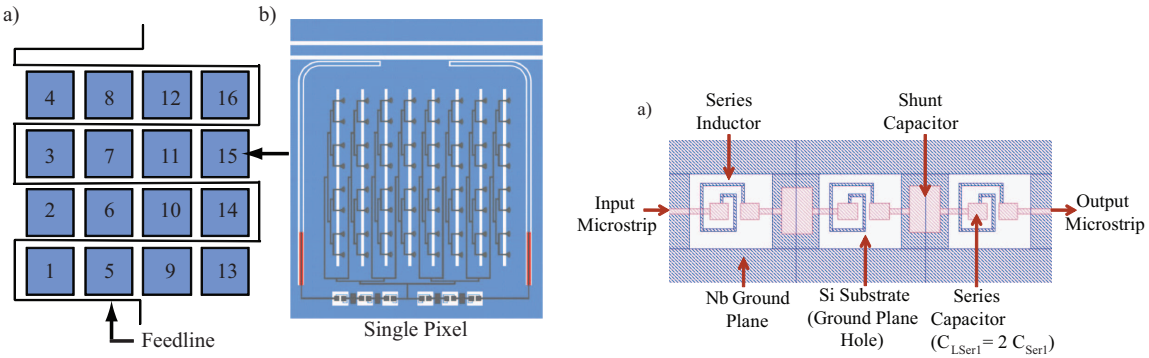

Figure 23. Left: The layout of a 4×4 array of dual-band pixels. Each pixel consists of a multislot antenna and an in-phase binary combining network; two on-chip filters that define the two bands centered at 230 GHz and 340 GHz; and two Nb/Al hybrid CPW resonators that serve as the detectors for the two bands. A common feedline is meandered past each pixel in the 4×4 array and simultaneously reads out all 32 detectors. **Right**: A close-up of the mm-wave bandpass filter design. The filter is a lumped-element design using spiral series inductors, and both series and shunt parallel-plate capacitors

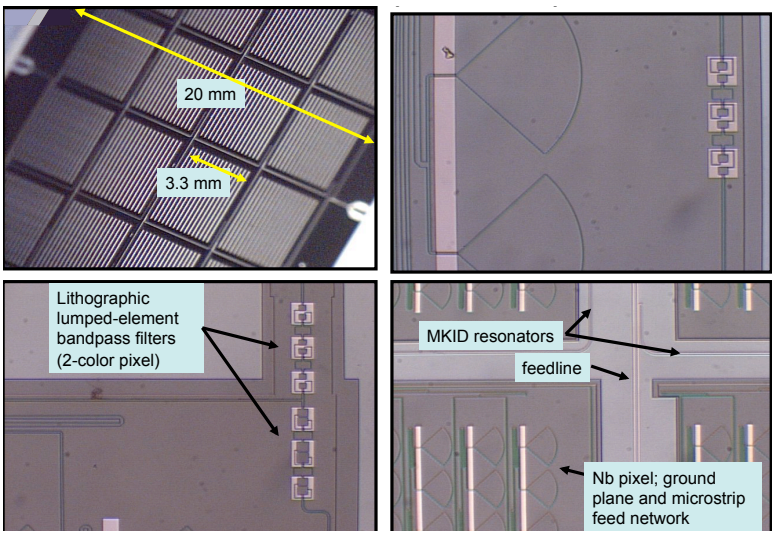

Figure 24. Microscope photographs of the 4×4 dual-band array. Each pixel is ~ 3.3 mm square. Microstrip radial stubs acting as mm-wave short circuits are used to couple the microstrip in-phase combining network to the slot antennas.

4.2. State of Maturity

A small camera was built and taken to the Caltech Submillimeter Observatory (CSO) in March 2007 in order to demonstrate the technology [163, 197]. The camera was based on a 4×4, dual-

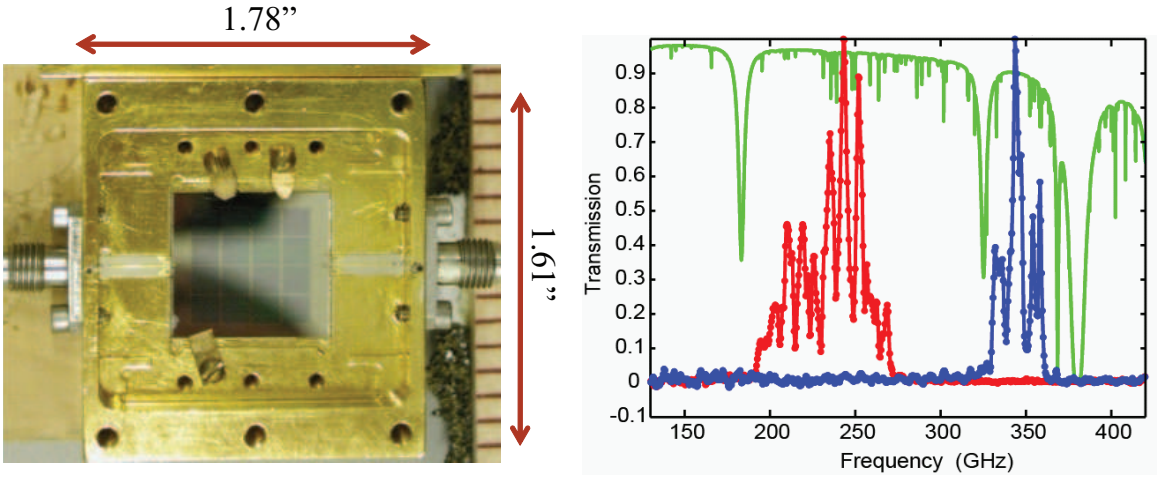

Figure 25. Left: The 4×4 array chip is mounted in a simple metal box. The input and output connections are wire-bonded to CPW to microstrip transitions fabricated on circuit boards, which are soldered to the center pins of the SMA/K coaxial connectors. **Right**: The frequency responses measured for a single dual-band pixel, indicating good agreement with the design values of the turn-on and turn-off frequencies of the on-chip filters. The lack of anti-reflection coatings on some of the optics may be causing the observed fringes; additional measurements are in progress.

band detector array as illustrated in Figures 23 and 24. The array chip was mounted into a simple housing (Fig. 25) and installed into a cryostat containing the optics and a 250 mK ^{3}He/^{3}He/^{4}He refrigerator. The frequency response was measured in the laboratory using a Fourier-transform spectrometer, which confirmed dual-band operation with the desired bandpasses (Fig. 25). The beam patterns were also measured in the laboratory and were found to generally agree with expectations. Using a digital readout system based on commercially available hardware [198], successful astronomical observations of bright objects (planets, HII regions) were made at the CSO, which again demonstrated the basic functionality of the system.

This quick ($\sim$ 6 month) exercise proved highly useful and revealed a number of significant issues. The resonators were found to be highly sensitive to the Earth's magnetic field, and this had a serious impact on the sensitivity achieved. A proper magnetic shield was subsequently designed and manufactured, and will be implemented for the next telescope demonstration. The physics of this effect is currently being investigated [199]; simple modifications to the resonator design may substantially reduce their magnetic field sensitivity. In addition, we have found that small field variations only affect the resonance frequency, so the problem could be circumvented using dissipation readout. A second issue was that the devices were found to be substantially overcoupled ($Q_c >> Q_i$), which again adversely impacts the sensitivity. This situation is now being investigated in detail and the lessons learned will be applied to the next version of the array design.

In order to verify the basic optical efficiency of the devices, measurements were performed in a laboratory dilution refrigerator cryostat containing a cryogenic blackbody. This setup has the advantage of having minimal optics between the detector and the source, and also has minimum levels of stray light. These results indicate that the overall efficiency is rather high, of order $\sim 50\%$.

The present situation can be summarized by saying that essentially all aspects of the basic physics of the detector operation have been confirmed and match expectations. In addition, a

fully-functional detector array incorporating antennas and on-chip filters has been demonstrated. However, the operation of a fully optimized array at the expected sensitivity in a complete system capable of astronomical observations is still a work in progress - we expect to reach this milestone in about a years' time

A much larger camera consisting of a 24×24 array of four-band pixels is now under construction (NSF ATI) for the CSO and is expected to be completed in mid-2010. One of the major tasks is the implementation of the 2304-channel readout electronics. We have studied the technical requirements in detail and have produced a specifications document. Our requirements are well within the state of the art, and we are currently in discussions with potential vendors for the development of a turnkey system.

4.3. Advantages and Disadvantages

The primary advantage of superconducting microresonator detectors is the relatively low cost for implementing a full system. This is due to several factors:

- Detector fabrication is very straightforward and fast, requiring only 3-6 levels of lithography depending on the design, and yields are high. Critical temperature (T_c) uniformity is not a significant issue. Film thickness uniformity is necessary at the $\sim 10\%$ level.
- The devices are already fully multiplexed and a separate complex multiplexer chip is not needed. In addition, procedures for attaching the detector array to a multiplexer array (using wire bonding, indium bump bonding, etc.) are not required.
- Compared to first-generation TDM/FDM SQUID multiplexing, much larger multiplexing factors ($\sim 10^3$ instead of $\sim 10^1$) are possible. This reduces the wire count dramatically.
- Microresonator detectors can be used as "drop-in" replacements for microstrip-coupled TES bolometers. This allows existing antenna designs, filter designs, etc. to be reused.

There are also several technical advantages. Perhaps the most useful is that the saturation characteristics are very benign. As the optical load is increased, the internal quality factor Q_i drops, and eventually no longer obeys the optimal coupling condition $Q_c = Q_i$. This just causes the amplifier noise contribution to increase - the detector remains functional with a graceful degradation of its performance. Another advantage is speed: leg-isolated bolometers will be several orders of magnitude slower for the same NEP. The low cost and ease of implementation also facilitates rapid development of the technology. Finally, superconducting microresonators are finding numerous applications in other areas of physics, and the research community in this area is growing rapidly.

The primary disadvantages are:

- Lower level of maturity. TES bolometer development has a $\sim$ 5-year head start.
- Sensitivity. Using dissipation readout and commonly available HEMT amplifiers, sensitivities around $2\times$ BLIP are achievable today, and somewhat better using state-of-the-art SiGe amplifiers. Comparable performance levels should also be possible with frequency readout along with emerging low-noise resonator designs. Reaching BLIP-level performance should eventually be possible but will likely take several more years of effort.
- Readout electronics are not yet available. A first-generation, 2k-channel FPGA-based readout electronics system should be ready by mid-2010. A low power dissipation readout system suitable for space will likely require eventual development of a custom ASIC; however this is best done after the signal processing schemes have been developed and demonstrated using FPGAs.

4.4. Technology Readiness Level

I judge the level to be around TRL4: a "low-fidelity" demonstration of a working system has been achieved (the demonstration camera on the CSO). I expect the TRL level to jump to 5-6 over the next several years; the milestone will be having the new large CSO camera working at its target performance. Prior to inclusion in a CMBpol mission proposal, one would also like to demonstrate dual-polarization versions working at the desired sensitivity levels in the laboratory.

References

[1] M. Ukibe, B. Belier, P. Chamus, C. Cobrea, L. Dumoulin, B. Fernandez, T. Fournier, O. Guillaudin, S. Marnieros, and S. Yates, "Fabrication of large NbSi bolometer arrays for CMB applications," *Nuc. Instr. and Meth. Phys. A*, vol. 559, p. 534, 2006.

[2] A. Orlando, M. Bruijn, H. Hoevers, P. Mauskopf, P. de Korte, E. Krouwer, and M. Ridder, "A waveguide-coupled millimetre-wave TES bolometer suitable for 2-D arrays," *Nucl. Instr. and Meth. A*, vol. 559, p. 534, 2006.

[3] M. D. Audley, D. Glowacka, D. J. Goldie, V. Tsaneva, S. Withington, P. K. Grimes, C. E. North, G. Yassin, L. Piccirillo, P. Ade, and R. V. Sudiwala, "Performance of microstrip-coupled TES bolometers with finline transitions," in *Society of Photo-Optical Instrumentation Engineers (SPIE) Conference Series*, ser. Society of Photo-Optical Instrumentation Engineers (SPIE) Conference Series, vol. 7020, Aug. 2008.

[4] M. Myers, P. Ade, K. Arnold, G. Engargiola, B. Holzapfel, A. Lee, R. O'Brient, P. Richards, A. Smith, H. Spieler, and H. Tran, "Antenna-coupled bolometer arrays using transition-edge sensors," *Nucl. Instr. and Meth. A*, vol. 559, p. 531, 2006.

[5] H. LeDuc, M. Kenyon, P. Day, M. Yun, and J. Bock, "Fabrication of antenna-coupled transition edge sensors for polarimeter applications," *Nucl. Instr. and Meth. A*, vol. 559, p. 459, 2006.

[6] C. Kuo, J. Bock, J. Bonetti, J. Brevik, G. Chattopadhyay, P. Day, S. Golwala, M. Kenyon, A. Lange, H. LeDuc, H. Nguyen, R. Ogburn, A. Orlando, A. Transgrud, A. Turner, G. Wang, and J. Zmuidzinas, "Antenna-Coupled TES Bolometer Arrays for CMB Polarimetry," *Proc. SPIE*, vol. 7020, p. 70201l, 2008.

[7] T. Stevenson, W.-T. Hsieh, G. Schneider, D. Travers, N. Cao, E. Wollack, M. Limon, and A. Kogut, "Building blocks for a polarimeter-on-a-chip," *Nucl. Instr. and Meth. A*, vol. 559, p. 611, 2006.

[8] T. Stevenson, D. Benford, C. Bennett, N. Cao, D. Chuss, K. Denis, W. Hsieh, A. Kogut, S. Moseley, J. Panek, G. Schneider, D. Travers, K. U-Yen, G. Voellmer, and E. Wollack, "Cosmic Microwave Background Polarization Detector with High Efficiency, Broad Bandwidth, and Highly Symmetric Coupling to Transition Edge Sensor Bolometers," *Journal of Low Temperature Physics*, vol. 151, p. 471, 2008.

[9] F. Herschel, "Experiments on the Refrangibility of the Invisible Rays of the Sun," *Philosophical Transactions*, p. 294, 1800.

[10] S. Langley, "The Bolometer," *Nature*, vol. 25, p. 14, 1881.

[11] A. Goetz, "The Possible Use of Superconductivity for Radiometric Purposes," *Phys. Rev.*, vol. 55, p. 1270, 1939.

[12] D. Andrews, J. Bruksch, W.F., W. Ziegler, and E. . Blanchard, "Superconducting Films as Radiometric Receivers," *Phys. Rev.*, vol. 59, p. 1045, 1941.

[13] D. Andrews, R. Milton, and W. DeSorro, "A Fast Superconducting Bolometer," *JOSA*, vol. 36, no. 9, p. 518, 1946.

[14] N. Fuson, "The Infra-Red Sensitivity of Superconducting Bolometers," *JOSA*, vol. 38, no. 10, p. 845, 1948.

[15] W. Boyle and J. Rodgers, K.F., "Performance Characteristics of a New Low-Temperature Bolometer," *JOSA*, vol. JOSA, no. 1, p. 66, 1959.

[16] F. Low, "Low-Temperature Germanium Bolometer," *JOSA*, vol. 51, no. 11, p. 1300, 1961.

[17] J. Clarke, P. Richards, and N.-H. Yeh, "Composite superconducting transition edge bolometer," *Appl. Phys. Lett.*, vol. 30, p. 664, 1977.

[18] J. Clarke, G. Hoffer, P. Richards, and N.-H. Yeh, "Superconductive Bolometers for Submillimeter Wavelengths," *J. Appl. Phys.*, vol. 48, no. 2, p. 4865, 1977.

[19] S. Wentworth and D. Neikirk, "The Transition-Edge Microbolometer (TREMBOL)," *Proc. SPIE*, vol. 1292, p. 148, 1990.

[20] A. Lee, P. Richards, S. Nam, B. Cabrera, and K. Irwin, "A superconducting bolometer with strong electrothermal feedback," *Appl. Phys. Lett.*, vol. 69, p. 1801, 1996.

[21] K. Irwin, "An application of electrothermal feedback for high resolution cryogenic particle detection," *Appl. Phys. Lett.*, vol. 66, p. 1998, 1995.

[22] H. Dewhurst, "A Rapid Bolometer Made By Sputtering On Thin Films," *Proc. Phys. Soc.*, vol. 39, no. 1, p. 39, 1926.

[23] W. Cannon and M. Chester, "Fast Carbon Bolometer for Observing Thermal Pulses," *Rev. Sci. Inst.*, vol. 38, no. 3, p. 318, 1967.

[24] R. De Waard and S. Weiner, "Miniature Optically Immersed Thermistor Bolometer Arrays," *Ap. Opt.*, vol. 6, no. 8, p. 1327, 1967.

[25] H. Drew and A. Sievers, "A ^{3}He-Cooled Bolometer for the Far Infrared," *Ap. Opt.*, vol. 8, no. 10, p. 2067, 1969.

[26] P. Downey, A. Jeffries, S. Meyer, R. Weiss, F. Cahner, J. Donnelly, W. Lindley, R. Mountain, and D. Silversmith, "Monolithic Silicon Bolometers," *Ap. Opt.*, vol. 23, no. 6, p. 910, 1984.

[27] R. Bachmann, H. Kirsch, and T. Geballe, "Low Temperature Silicon Thermometer and Bolometer," *Rev. Sci. Inst.*, vol. 41, no. 4, p. 547, 1970.

[28] R. Britt and P. Richards, "An Adiabatic Demagnetization Refrigerator For Infrared Bolometers," *IJIMW*, vol. 2, no. 6, p. 1083, 1981.

[29] L. Lesyna, T. Roellig, and P. Kittel, "Bolometers Operated At 0.1 K And 0.2 K Cooled By Adiabatic Demagnetization," *IJIMW*, vol. 5, no. 6, p. 755, 1984.

[30] J. Mees, M. Nahum, and P. Richard, "New Designs for Antenna-coupled Superconducting Bolometers," *Appl. Phys. Lett.*, vol. 59, no. 18, p. 2329, 1991.

[31] J. Milatz and H. Van Der Velden, "Natural Limit of Measuring Radiation with a Bolometer," *Physica*, vol. X, no. 6, p. 24, 1943.

[32] B. H. Billings, W. L. Hyde, and E. E. Barr, "An investigation of the properties of evaporated metal bolometers," *Journal of the Optical Society of America (1917-1983)*, vol. 37, pp. 123–+, Mar. 1947.

[33] R. C. Jones, "Steady-state load curves for semi-conductor bolometers," *Journal of the Optical Society of America (1917-1983)*, vol. 36, pp. 448–+, Aug. 1946.

[34] ——, "The ultimate sensitivity of radiation detectors," *Journal of the Optical Society of America (1917-1983)*, vol. 37, pp. 879–+, Nov. 1947.

[35] R. Jones, "Factors of Merit for Radiation Detectors," *JOSA*, vol. 39, no. 8, p. 344, 1949.

[36] ——, "General Theory of Bolometer Performance," *JOSA*, vol. 43, no. 1, p. 1, 1953.

[37] J. Mather, "Bolometer noise: nonequilibrium theory," *Ap. Opt.*, vol. 21, no. 6, p. 1125, 1982.

[38] Y. Urano, "An Equivalent Circuit of a Bolometer," *J. Phys. Soc. Japan*, vol. 10, no. 10, p. 864, 1966.

[39] N. Fuson, "The Effect of Current Magnitude upon the Behavior of a Superconducting Bolometer n Its Transition Region," *J. App. Phys.*, vol. 30, p. 59, 1949.

[40] B. Lalevic, "Criteria for the Choice of a Superconducting Bolometer," *J. App. Phys.*, vol. 31, no. 7, p. 1234, 1960.

[41] M. Maul and M. Strandberg, "Equivalent Circuit of a Superconducting Bolometer," *J. Appl. Phys.*, vol. 40, no. 7, p. 2822, 1969.

[42] M. K. Maul, M. W. Strandberg, and R. L. Kyhl, "Excess Noise in Superconducting Bolometers," *Physical Review*, vol. 182, pp. 522–525, Jun. 1969.

[43] C. Bertin and K. Rose, "Comparison of Superconducting and Semiconducting Bolometers," *J. App. Phys.*, vol. 42, no. 1, p. 163, 1971.

[44] S. Tinchev, L. Bliek, and V. Kose, "A Consistent Model For 1/f-Noise In Thin-Film Devices Such As Bolometers, Josephson Junctions And Squids," *Phys. Lett.*, vol. 94A, no. 8, p. 381, 1983.

[45] C. Knoedler, "Phase-Slip Shot Noise Contribution to Excess Noise of Superconducting Bolometers," *J. Appl. Phys.*, vol. 54, no. 5, p. 2773, 1983.

[46] R. Sherlock and A. Wyatt, "The effect of self-heating on the dynamical response of bolometric detectors," *J. Phys. E: Sci. Instrum.*, vol. 16, p. 669, 1983.

[47] G. C. Irwin, K. D. & Hilton, *"Transition-Edge Sensors"*, C. Enss, Ed. Springer-Verlag, 2005, vol. Cryogenic Particle Detecion.

[48] B. Cabrera, "Introduction to TES Physics," *J. Low Temp. Phys.*, vol. 151, p. 82, 2008.

[49] M. Lindeman, K. Barger, D. Brandl, S. Crowder, L. Rocks, D. McCammon, and H. Hoevers, "The Superconducting Transition in 4-D: Temperature, Current, Resistance and Heat Capacity," *J. Low Temp. Phys.*, vol. 151, p. 190, 2008.

[50] K. Irwin, "Thermodynamics of nonlinear bolometers near equilibrium," *Nuclear Instruments and Methods in Physics Research A*, vol. 559, p. 718, 2006.

[51] D. McCammon, *"Thermal Equilibrium Calorimeters – An Introduction", in Cryogenic Particle Detection*, C. Enss, Ed. Springer-Verlag, 2005.

[52] S.-F. Lee, J. M. Gildemeister, W. Holmes, A. T. Lee, and P. L. Richards, "Voltage-Biased Superconducting Transition-Edge Bolometer with Strong Electrothermal Feedback Operated at 370 mK," *Applied Optics*, vol. 37, pp. 3391–3397, Jun. 1998.

[53] J. Gilemeister, A. Lee, and P. Richards, "A fully lithographed voltage-biased superconducting spiderweb bolometer," *APL*, vol. 74, no. 6, p. 868, 1999.

[54] ——, "Monolithic arrays of absorber-coupled voltage-biased superconducting bolometers," *APL*, vol. 77, no. 24, p. 4040, 2000.

[55] ——, "Model for excess noise in voltage-biased superconducting bolometers," *Ap. Opt*, vol. 40, no. 34, p. 6229, 2001.

[56] R. Romani, A. Miller, B. Cabrera, E. Figueroa-Feliciano, and S. Nam, "First Astronomical Application Of A Cryogenic Transition Edge Sensor Spectrophotometer," *Ap.J.*, vol. 521, p. L153, 1999.

[57] D. Benford, C. Allen, J. Chervenak, E. Grossman, K. Irwin, A. Kutyrev, M. J.M., S. Moseley, R. Shafer, and C. Reintsema, "Superconducting Bolometer Arrays for Submillimeter Astronomy," in *APS Conference*, vol. 217, 2000, p. 134.

[58] D. Benford, "Multiplexed Readout of Superconducting Bolometers," *IJIMW*, vol. 21, no. 12, p. 1909, 2000.

[59] J. Staguhn, C. Allen, D. Benford, J. Chervenak, M. Freund, S. Khan, A. Kutyrev, S. Moseley, R. Shafer, S. Deiker, E. Grossman, G. Hilton, K. Irwin, J. Martinis, S. Nam, D. Rudman, and D. Wollman, "TES Detector Noise Limited Readout Using SQUID Multiplexers," in *AIP Conference proceedings*, vol. 605, 2001, p. 321.

[60] J. Staguhn, S. Moseley, D. Benford, C. Allen, J. Chervenak, T. Stevenson, and W.-T. Hsieh, "Approaching the fundamental noise limit in Mo/Au TES bolometers with

transverse normal metal bars," *Nuclear Instruments and Methods in Physics Research A*, vol. 520, p. 336, 2004.

[61] D. Benford, S. Moseley, J. Staguhn, C. Allen, J. Chervenak, T. Stevenson, and W.-T. Hsieh, "Parameter Comparison for Low-Noise Mo/Au TES Bolometers," *Nuclear Instruments and Methods in Physics Research A*, vol. 520, p. 270, 2004.

[62] D. Benford, C. Ames, T.A., E. J.A., Grossman, K. Irwin, S. Khan, B. Maffei, S. Moseley, F. Pajot, T. Phillips, J.-C. Renault, C. Reintsema, C. Rioux, R. Shafer, J. Staguhn, C. Vastel, and G. Voellmer, "First Astronomical Use of Multiplexed Transition Edge Bolometers," in *AIP Conference proceedings*, vol. 605, 2001, p. 589.

[63] D. Benford, J. Staguhn, T. Ames, C. Allen, J. Chervenak, C. Kennedy, S. Lefranc, S. Maher, S. Moseley, F. Pajot, C. Rioux, R. Shafer, and G. Voellmer, "First astronomical images with a multiplexed superconducting bolometer array," *Proc. SPIE*, vol. 6275, p. 62751C, 2006.

[64] T. Saab, E. Apodacas, S. Bandler, K. Boyce, J. Chervenak, E. Figueroa-Feliciano, F. Finkbeiner, C. Hammock, R. Kelley, M. Lindeman, F. Porter, and C. Stahle, "Characterization and Modeling of Transition Edge Sensors for High Resolution X-ray Calorimeter Arrays," *Nucl. Instr. and Meth. A*, vol. 520, p. 281, 2003.

[65] M. Lindeman, S. Bandler, S. Brekosky, J. Chervenak, E. Figueroa-Feliciano, F. Finkbeiner, T. Saab, and C. Stahle, "Characterization and Reduction of Noise in Mo/Au Transition Edge Sensors," *Nucl. Instr. and Meth. A*, vol. 520, p. 348, 2003.

[66] S. Bandler, E. Figueroa-Feliciano, C. Stahle, K. Boyce, R. Brekosky, J. Chervenak, F. Finkbeiner, R. Kelley, M. Lindeman, F. Porter, and T. Saab, "Design of Transition Edge Sensor Microcalorimeters for Optimal Performance," *Nucl. Instr. and Meth. A*, vol. 520, p. 285, 2003.

[67] J. Chervenak, K. Irwin, E. Grossman, J. Martinis, C. Reintsema, and M. Huber, "Superconducting multiplexer for arrays of transition edge sensors," *App. Phys. Lett.*, vol. 74, no. 26, p. 4043, 1999.

[68] K. Irwin, "SQUID Multiplexers for Transition-Edge Sensors," *Physica C*, vol. 368, p. 203, 2002.

[69] K. Irwin, M. Audley, J. Beall, J. Beyer, S. Deiker, W. Doriese, W. Duncan, G. Hilton, W. Holland, C. Reintsema, J. Ullom, L. Vale, and Y. Xu, "In-Focal-Plane SQUID Multiplexer," *Nucl. Instr. and Meth. A*, vol. 520, p. 544, 2004.

[70] J. Staguhn, D. Benford, J. Chervenak, J. Moseley, S.H., C. Allen, T. Stevenson, and W.-T. Hsieh, "Design techniques for improved noise performance of superconducting Transition Edge Sensor bolometers," *Proc. SPIE*, vol. 5498, p. 390, 2004.

[71] J. Ullom, W. Doriese, G. Hilton, J. Beall, S. Deiker, W. Duncan, L. Ferreira, K. Irwin, C. Reintsema, and L. Vale, "Characterization and reduction of unexplained noise in superconducting transition-edge sensors," *App. Phys. Lett.*, vol. 84, no. 21, p. 4206, 2004.

[72] S. R. Dicker, P. A. Ade, D. J. Benford, M. J. Devlin, K. D. Irwin, P. R. Jewell, B. S. Mason, S. H. Moseley, M. P. Supanich, and C. Tucker, "A 90-GHz array for use on the Green Bank Telescope," in *Society of Photo-Optical Instrumentation Engineers (SPIE) Conference Series*, ser. Society of Photo-Optical Instrumentation Engineers (SPIE) Conference Series, J. M. Oschmann, Jr., Ed., vol. 5489, Oct. 2004, pp. 1221–1229.

[73] D. Benford, S. Dicker, E. Wollack, M. Supanich, J. Staguhn, S. Moseley, K. Irwin, M. Devlin, J. Chervenak, and T. Chen, "A planar two-dimensional superconducting bolometer array for the Green Bank Telescope," *Proc. SPIE*, vol. 5498, p. 208, 2004.

[74] A. Kosowsky, "The Atacama Cosmology Telescope," *New Astronomy Reviews*, vol. 47, p. 939, 2003.

[75] M. Niemack and the ACT Collaboration, "Measuring two-millimeter radiation with a prototype multiplexed TES receiver for ACT," *Proc. SPIE*, vol. 6275, p. 62750C, 2006.

[76] D. Benford, J. Staguhn, G. Stacey, L. Page, S. Moseley, K. Irwin, J. Chervenak, and C. Allen, "Design and Fabrication of Two-Dimensional Superconducting Bolometer Arrays," *Proc. SPIE*, vol. 5498, p. 647, 2004.

[77] C. Hunt, J. Bock, P. Day, A. Goldin, A. Lange, H. LeDuc, A. Vayonakis, and J. Zmuidzinas, "Transition-edge superconducting antenna-coupled bolometer," *Proc. SPIE*, vol. 4855, p. 318, 2003.

[78] A. Goldin, J. J. Bock, A. E. Lange, H. Leduc, A. Vayonakis, and J. Zmuidzinas, "Antennas for bolometric focal plane," *Nuclear Instruments and Methods in Physics Research A*, vol. 520, pp. 390–392, Mar. 2004.

[79] P. Day, H. LeDuc, A. Golding, C. Dowell, and J. Zmuidzinas, "Far Infrared/ Submillimeter Imager-Polarimeter Using Distributed Antenna-Coupled Transition Edge Sensors," *Proc. SPIE*, vol. 5498, p. 857, 2004.

[80] M. Myers, W. Holzapfel, A. Lee, R. O'Brient, P. Richards, D. Schwan, A. Smith, H. Spieler, and H. Tran, "Arrays of Antenna-Coupled Bolometers using Transition Edge Sensors," *Nucl. Instr. and Meth. A*, vol. 520, p. 424, 2003.

[81] M. Dobbs, N. Halverson, P. Ade, K. Basu, A. Beelen, F. Bertoldi, C. Cohalan, H. Cho, R. Güsten, W. Holzapfel, Z. Kermish, R. Kneissl, A. Kovács, E. Kreysa, T. Lanting, A. Lee, M. Lueker, J. Mehl, K. Menten, D. Muders, M. Nord, T. Plagge, P. Richards, P. Schilke, D. Schwan, H. Spieler, A. Weiss, and M. White, "APEX-SZ first light and instrument status," *New Astronomy Reviews*, vol. 50, no. 11-12, p. 960, 2006.

[82] K. D. Irwin, "The Thermodynamics of Nonlinear Bolometers Near Equilibrium," in *TES III, Gainesville, FL*, August 17-18, 2006.

[83] H. Hoevers, "Thermal physics of transition edge sensor arrays," *Nucl. Instr. and Meth. A*, vol. 559, p. 702, 2006.

[84] M. Bruijn, A. Germeau, H. Hoevers, P. de Korte, J. van der Kuur, and M. Ridder, "Steepness, noise and instabilities of Ti/Au transition edge thermometers," *Nucl. Instr. and Meth. A*, vol. 559, p. 709, 2006.

[85] H. Hoevers, M. Bruijn, L. Dirks, B.P.F. adn Gottardi, P. de Korte, J. van der Kuur, A. Popescu, M. Ridder, Y. Takei, and D. Takken, "Comparative Study of TiAu-Based TES Microcalorimeters with Different Geometries," *Journal of Low Temperature Physics*, vol. 151, p. 94, 2008.

[86] G. W. Fraser, "On the nature of the superconducting-to-normal transition in transition edge sensors," *Nuclear Instruments and Methods in Physics Research A*, vol. 523, p. 234, 2004.

[87] M. Galeazzi, "Flux Flow Noise in Transition Edge Sensors," in *TES III, Gainesville, FL*, August 17-18, 2006.

[88] M. Lindeman, M. Anderson, S. Bandler, N. Bilgri, J. Chervenak, S. Gwynne Crowder, S. Fallows, E. Figueroa-Feliciano, F. Finkbeiner, N. Iyomoto, R. Kelley, C. Kilbourne, T. Lai, J. Man, D. McCammon, K. Nelms, F. Porter, L. Rocks, T. Saab, J. Sadleir, and G. Vidugiris, "Percolation model of excess electrical noise in transition-edge sensors," *Nuclear Instruments and Methods in Physics Research A*, vol. 559, p. 715, 2006.

[89] H. Hoevers, A. Bento, M. Bruijn, L. Gottardi, M. Korevaar, W. Mels, and P. de Korte, "Thermal fluctuation noise in a voltage biased superconducting transition edge thermometer," *Applied Physics Letters*, vol. 77, p. 4422, 2000.

[90] A. Luukanen, K. M. Kinnunen, A. K. Nuottajaumlrvi, H. F. Hoevers, W. M. Bergmann Tiest, and J. P. Pekola, "Fluctuation-Limited Noise in a Superconducting Transition-Edge Sensor," *Physical Review Letters*, vol. 90, p. 238306, 2003.

[91] S. Crowder, M. Lindeman, M. Anderson, S. Bandler, N. Bilgri, M. Bruijn, J. Chervenak, E. Figueroa-Feliciano, F. Finkbeiner, A. Germeau, H. Hoevers, N. Iyomoto, R. Kelly, C. Kilbourne, T. Lai, J. Man, D. McCammon, K. Nelms, F. Porter, L. Rocks, T. Saab, J. Sadleir, and G. Vidugiris, "An investigation of excess noise in transition-edge sensors on a solid silicon substrate," *Nucl.Instr.and Meth.A*, vol. 559, p. 721, 2006.

[92] D. Brandt, G. Fraser, and S. Smith, "Excess Noise in TESs – A Comparison Between Theories," in *TES III, Gainesville, FL*, August 17-18, 2006.

[93] K. Kinnunen, A. Nuottajärvi, and I. Maasilta, "A Transition-Edge Sensor with Two Excess Noise Mechanisms," *Journal of Low Temperature Physics*, vol. 151, p. 144, 2008.

[94] E. Barrentine, P. Timbie, T. Stevenson, S. Ali, J. Chervenak, E. Wollack, S. Moseley, C. Allen, W. Hseih, T. Miller, D. Benford, and A. Brown, "Sensitivity Measurements of a Transition-Edge Hot-Electron Microbolometer for Millimeter-Wave Astrophysical Observations," *Journal of Low Temperature Physics*, vol. 151, p. 173, 2008.

[95] K. M. Kinnunen, A. K. Nuottajärvi, J. Leppäniemi, and I. J. Maasilta, "Reducing Excess Noise in Au/Ti Transition-Edge Sensors," *Journal of Low Temperature Physics*, vol. 151, p. 119, 2008.

[96] M. Griffin, J. Bock, and W. Gear, "Relative performance of filled and feedhorn-coupled focal-plane architectures," *Ap. Opt.*, vol. 41, no. 31, p. 6543, 2002.

[97] D. J. Benford, G. M. Voellmer, J. A. Chervenak, K. D. Irwin, S. H. Moseley, R. A. Shafer, and J. G. Staguhn, "Design and fabrication of a 2D superconducting bolometer array for SAFIRE," *Proc. SPIE*, vol. 4857, p. 125, 2003.

[98] C. Bradford, M. Kenyon, W. Holmes, J. Bock, T. Koch, and the BLISS study team, "Sensitive far-IR survey spectroscopy: BLISS for SPICA," *Proc. SPIE*, vol. 7020, p. 70201O, 2008.

[99] M. Kenyon, P. Day, C. Bradford, J. Bock, and H. LeDuc, "Electrical Properties of Background-Limited Membrane-Isolation Transition-Edge Sensing Bolometers for Far-IR/Submillimeter Direct-Detection Spectroscopy," *J. Low Temp. Phys.*, vol. 151, p. 112, 2008.

[100] P. Mauskopf, D. Morozov, D. Glowacka, D. Goldie, S. Withington, M. Bruijn, P. DeKorte, H. Hoevers, M. Ridder, J. Van Der Kuur, and J.-R. Gao, "Development of transition edge superconducting bolometers for the SAFARI Far-Infrared spectrometer on the SPICA space-borne telescope," *Proc. SPIE*, vol. 7020, p. 70200N, 2008.

[101] B. Karasik, D. Olaya, J. Wei, S. Pereverzev, M. Gershenson, J. Kawamura, W. McGrath, and A. Sergeev, "Record-Low NEP in Hot-Electron Titanium Nanobolometers," *IEEE Trans. App. Superconductivity*, vol. 17, no. 2, p. 293, 2007.

[102] J. Wei, D. Olaya, B. Karasik, S. Pereverzev, A. Sergeev, and M. Gershenson, "Ultra-Sensitive Hot-Electron Nanobolometers for Terahertz Astrophysics," *astro-ph*, p. 0710.5474, 2007.

[103] T. Marriage, J. Chervenak, and W. Doriese, "Testing and assembly of the detectors for the Millimeter Bolometer Array Camera on ACT," *Nucl. Instr. and Meth. A*, vol. 559, p. 551, 2006.

[104] M. Niemack, Y. Zhao, E. Wollack, R. Thornton, E. Switzer, D. Swetz, S. Staggs, L. Page, O. Sytrzak, S. Moseley, T. Marriage, M. Limon, J. Lau, J. Klein, M. Kaul, N. Jarosik, K. Irwin, A. Hincks, G. Hilton, M. Halpern, R. Fowler, J.W.and Fisher, R. Dünner,

W. Doriese, S. Dicker, M. Devlin, J. Chervenak, B. Burger, E. Battistelli, J. Appel, M. Amiri, C. Allen, and A. Aboobaker, "A Kilopixel Array of TES Bolometers for ACT: Development, Testing, and First Light," *J. Low Temp. Phys.*, vol. 151, p. 690, 2008.

[105] J. Fowler, "The Atacama Cosmology Telescope: 2007 Initial Observations," in *Aspen Conference on the Cosmic Microwave Background Radiation*, January 28, 2008.

[106] P. Korngut, S. Dicker, B. Mason, P. Ade, J. Aguirre, T. Ames, D. Benford, J. Chervenak, T. Chen, M. Compiegne, W. Cotton, M. Devlin, E. Figueroa-Feliciano, K. Irwin, S. Maher, P. Martin, M. Mello, S. Moseley, C. Tucker, J. Staguhn, B. Werner, and S. D. White, "High Resolution Continuum Observations Of The Orion Nebula At 3.3mm With MUSTANG And The GBT," *BAAS*, vol. 53.01, no. 40, p. 249, 2008.

[107] J. Staguhn, C. Allen, D. Benford, E. Sharp, T. Ames, R. Arendt, D. Chuss, E. Dwek, A. Kovacs, S. Maher, C. Marx, T. Miller, S. Moseley, S. Navaroo, A. Sievers, G. Voellmer, and E. Wollack, "GISMO, a 2 mm Bolometer Camera Optimized for the Study of High Redshift Galaxies," *J. Low Temp. Phys.*, vol. 151, p. 709, 2008.

[108] J. Staguhn, D. Benford, C. Allen, S. Moseley, E. Sharp, T. Ames, W. Brunswig, D. Chuss, E. Dwek, S. Maher, C. Marx, T. Miller, S. Navarro, and E. Wollack, "GISMO: A 2-Millimeter Bolometer Camera for the IRAM 30 m Telescope," *Proc. SPIE*, vol. 6275, p. 62751D, 2006.

[109] C. Allen, D. Benford, T. Miller, S. Moseley, J. Staguhn, and E. Wollack, "Design and Fabrication Highlights Enabling a 2 mm,128 Element Bolometer Array for GISMO," *J. Low Temp. Phys.*, vol. 151, p. 266, 2008.

[110] G. Bernstein, "Advanced Exposure-Time Calculations: Undersampling, Dithering, Cosmic Rays, Astrometry, and Ellipticities," *PASP*, vol. 114, p. 98, 2002.

[111] C. Allen, D. Benford, J. Chervenak, D. Chuss, T. Miller, S. Moseley, J. Staguhn, and E. Wollack, "Backshort-Under-Grid arrays for infrared astronomy," *Nucl. Instr. and Meth. A,*, vol. 559, p. 522, 2008.

[112] J. G. Staguhn, C. A. Allen, D. J. Benford, J. A. Chervenak, D. T. Chuss, T. M. Miller, S. H. Moseley, and E. J. Wollack, "Characterization of TES bolometers used in 2-dimensional Backshort-Under-Grid (BUG) arrays for far-infrared astronomy," *Nuclear Instruments and Methods in Physics Research A*, vol. 559, pp. 545–547, Apr. 2006.

[113] C. Allen, J. Abrahams, D. Benford, J. Chervenak, D. Chuss, J. Staguhn, T. Miller, S. Moseley, and E. Wollack, "Far infrared through millimeter Backshort-Under-Grid arrays," *Proc. SPIE*, vol. 6275, p. 62750B, 2006.

[114] T. Miller, J. Abrahams, and C. Allen, "Fabricating interlocking support walls, with an adjustable backshort, in a TES bolometer array for far-infrared astronomy," *Nucl. Instr. and Meth. A*, vol. 559, p. 548, 2006.

[115] J. Vieira, "The South Pole Telescope," in *Aspen Conference on the Cosmic Microwave Background Radiation*, 2008.

[116] A. Taylor, "Clover – A B-mode polarization experiment," *NAR*, vol. 50, p. 993, 2006.

[117] M. Audley, R. Barker, M. Crane, R. Dace, D. Glowacka, D. Goldie, A. Lasenby, H. Stevenson, V. Tsaneva, S. Withington, P. Grimes, B. Johnson, G. Yassin, L. Piccirillo, W. Pisano, G.and Duncan, G. Hilton, K. Irwin, C. Reintsema, and M. Halpern, "TES imaging array technology for CLOVER," *Proc. SPIE*, vol. 6275, p. 627524, 2006.

[118] G. Siringo, A. Weiß, E. Kreysa, F. Schuller, and A. Kovacs, "SABOCA Technical Verification Report," APEX memo., Tech. Rep., 2008.

[119] W. Holland, M. MacIntosh, A. Fairley, D. Kelly, D. Montgomery, D. Gostick, E. Atad-Ettedgui, M. Ellis, I. Robson, M. Hollister, A. Woodcraft, P. Ade, I. Walker, K. Irwin,

G. Hilton, W. Duncan, C. Reintsema, A. Walton, W. Parkes, C. Dunare, M. Fich, J. Kycia, M. Halpern, D. Scott, A. Gibb, J. Molnar, E. Chapin, D. Bintley, S. Craig, T. Chylek, T. Jenness, F. Economou, and G. Davis, "SCUBA-2: a 10,000-pixel submillimeter camera for the James Clerk Maxwell Telescope," *Proc. SPIE*, vol. 6275, p. 62751E, 2006.

[120] (2008) JCMT Newsletter #28 (Spring '08). [Online]. Available: `http://www.jach.hawaii.edu/JCMT/publications/newsletter/n28/jcmt-n28.pdf`

[121] P. Oxley, P. Ade, C. Baccigalupi, P. deBernardis, H.-M. Cho, M. Devlin, S. Hanany, B. Johnson, T. Jones, A. Lee, T. Matsumura, A. Miller, M. Milligan, T. Renbarger, H. Spieler, R. Stompor, G. Tucker, and M. Zaldarriaga, "The EBEX experiment," *Proc.SPIE*, vol. 5543, p. 320, 2004.

[122] B. Reichborn-Kjennerud, "EBEX: E and B EXperiment: A CMB Polarization Experiment," in *Aspen Conference on the Cosmic Microwave Background Radiation*, 2008.

[123] T. E. Montroy, P. A. R. Ade, R. Bihary, J. J. Bock, J. R. Bond, J. Brevik, C. R. Contaldi, B. P. Crill, A. Crites, O. Doreacute, L. Duband, S. R. Golwala, M. Halpern, G. Hilton, W. Holmes, V. V. Hristov, K. Irwin, W. C. Jones, C. L. Kuo, A. E. Lange, C. J. MacTavish, P. Mason, J. Mulder, C. B. Netterfield, E. Pascale, J. E. Ruhl, A. Trangsrud, C. Tucker, A. Turner, and M. Viero, "SPIDER: a new balloon-borne experiment to measure CMB polarization on large angular scales," *Proc. SPIE*, vol. 6267, p. 62670R, 2006.

[124] C. Hunt, J. Bock, P. Day, A. Goldin, A. Lange, H. LeDuc, A. Vayonakis, and J. Zmuidzinas, "Transition-edge superconducting antenna-coupled bolometer," *Proc. SPIE*, vol. 4855, p. 318, 2003.

[125] [Online]. Available: `http://en.wikipedia.org/wiki/Spider_CMB`

[126] C. MacTavish, "Spider Optimization: Probing the Systematics of a B-Mode Experiment," January 2008, Aspen Conference on the Cosmic Microwave Background Radiation, January 29, 2008.

[127] D. Benford, S. Moseley, G. Stacey, R. Shafer, and J. Staguhn, "Far-infrared imaging spectroscopy with SAFIRE on SOFIA," *Proc.SPIE*, vol. 4857, p. 105, 2003.

[128] C. Allen, D. Benford, T. Miller, J. Moseley, S.H.and Staguhn, and E. Wollack, "Technology developments toward large format long wavelength bolometer arrays," *Proc. SPIE*, vol. 6678, p. 667806, 2007.

[129] D. J. Benford, J. G. Staguhn, S. H. Moseley, C. A. Allen, J. A. Chervenak, K. D. Irwin, S. R. Dicker, M. J. Devlin, T. Nikola, T. E. Oberst, and G. J. Stacey, "Superconducting Bolometers for Submillimeter Spectroscopy from Ground-Based, Airborne, and Space Platforms," in *ASPC:From Z-Machines to ALMA: (Sub)Millimeter Spectroscopy of Galaxies*, vol. 375, 2007, p. 217.

[130] J. Mankins, "Technology Readiness Levels," NASA Office of Space Access and Technology, Tech. Rep., 1995.

[131] [Online]. Available: `http://www.hq.nasa.gov/office/codeq/trl/trlchrt.pdf`

[132] F. Menanteau and J. P. Hughes, "Southern Cosmology Survey II: Physical Properties of SZE-Selected Galaxy Clusters," *ArXiv e-prints*, Nov. 2008.

[133] Z. Staniszewski, P. A. R. Ade, K. A. Aird, B. A. Benson, L. E. Bleem, J. E. Carlstrom, C. L. Chang, H. . Cho, T. M. Crawford, A. T. Crites, T. de Haan, M. A. Dobbs, N. W. Halverson, G. P. Holder, W. L. Holzapfel, J. D. Hrubes, M. Joy, R. Keisler, T. M. Lanting, A. T. Lee, E. M. Leitch, A. Loehr, M. Lueker, J. J. McMahon, J. Mehl, S. S. Meyer, J. J. Mohr, T. E. Montroy, C. . Ngeow, S. Padin, T. Plagge, C. Pryke, C. L. Reichardt, J. E. Ruhl, K. K. Schaffer, L. Shaw, E. Shirokoff, H. G. Spieler, B. Stalder, A. A. Stark, K. Vanderlinde, J. D. Vieira, O. Zahn, and A. Zenteno, "Galaxy clusters discovered with a Sunyaev-Zel'dovich effect survey," *ArXiv e-prints*, Oct. 2008.

[134] J. C. Mather, E. S. Cheng, D. A. Cottingham, R. E. Eplee, Jr., D. J. Fixsen, T. Hewagama, R. B. Isaacman, K. A. Jensen, S. S. Meyer, P. D. Noerdlinger, S. M. Read, L. P. Rosen, R. A. Shafer, E. L. Wright, C. L. Bennett, N. W. Boggess, M. G. Hauser, T. Kelsall, S. H. Moseley, Jr., R. F. Silverberg, G. F. Smoot, R. Weiss, and D. T. Wilkinson, "Measurement of the cosmic microwave background spectrum by the COBE FIRAS instrument," *Astrophysical Journal*, vol. 420, pp. 439–444, Jan. 1994.

[135] J. Mather, "Bolometers: ultimate sensitivity, optimization, and amplifier coupling," *Ap. Opt*, vol. 23, p. 584, 1984.

[136] J. J. Bock, D. Chen, P. D. Mauskopf, and A. E. Lange, "A Novel Bolometer for Infrared and Millimeter-Wave Astrophysics," *Space Science Reviews*, vol. 74, pp. 229–235, Oct. 1995.

[137] Y. D. Takahashi, D. Barkats, J. O. Battle, E. M. Bierman, J. J. Bock, H. C. Chiang, C. D. Dowell, E. F. Hivon, W. L. Holzapfel, V. V. Hristov, W. C. Jones, J. P. Kaufman, B. G. Keating, J. M. Kovac, C.-L. Kuo, A. E. Lange, E. M. Leitch, P. V. Mason, T. Matsumura, H. T. Nguyen, N. Ponthieu, G. M. Rocha, K. W. Yoon, P. Ade, and L. Duband, "CMB polarimetry with BICEP: instrument characterization, calibration, and performance," in *Society of Photo-Optical Instrumentation Engineers (SPIE) Conference Series*, ser. Society of Photo-Optical Instrumentation Engineers (SPIE) Conference Series, vol. 7020, Aug. 2008.

[138] C. D. Dowell, C. A. Allen, R. S. Babu, M. M. Freund, M. Gardner, J. Groseth, M. D. Jhabvala, A. Kovacs, D. C. Lis, S. H. Moseley, Jr., T. G. Phillips, R. F. Silverberg, G. M. Voellmer, and H. Yoshida, "SHARC II: a Caltech submillimeter observatory facility camera with 384 pixels," in *Society of Photo-Optical Instrumentation Engineers (SPIE) Conference Series*, ser. Society of Photo-Optical Instrumentation Engineers (SPIE) Conference Series, T. G. Phillips and J. Zmuidzinas, Eds., vol. 4855, Feb. 2003, pp. 73–87.

[139] J. Glenn, P. A. R. Ade, M. Amarie, J. J. Bock, S. F. Edgington, A. Goldin, S. Golwala, D. Haig, A. E. Lange, G. Laurent, P. D. Mauskopf, M. Yun, and H. Nguyen, "Current status of Bolocam: a large-format millimeter-wave bolometer camera," in *Society of Photo-Optical Instrumentation Engineers (SPIE) Conference Series*, ser. Society of Photo-Optical Instrumentation Engineers (SPIE) Conference Series, T. G. Phillips and J. Zmuidzinas, Eds., vol. 4855, Feb. 2003, pp. 30–40.

[140] M. J. Devlin, P. A. R. Ade, I. Aretxaga, J. J. Bock, J. Chung, E. Chapin, S. R. Dicker, M. Griffin, J. Gundersen, M. Halpern, P. Hargrave, D. Hughes, J. Klein, G. Marsden, P. Martin, P. D. Mauskopf, B. Netterfield, L. Olmi, E. Pascale, M. Rex, D. Scott, C. Semisch, M. Truch, C. Tucker, G. Tucker, A. D. Turner, and D. Weibe, "The Balloon-borne Large Aperture Submillimeter Telescope (BLAST)," in *Society of Photo-Optical Instrumentation Engineers (SPIE) Conference Series*, ser. Society of Photo-Optical Instrumentation Engineers (SPIE) Conference Series, C. M. Bradford, P. A. R. Ade, J. E. Aguirre, J. J. Bock, M. Dragovan, L. Duband, L. Earle, J. Glenn, H. Matsuhara, B. J. Naylor, H. T. Nguyen, M. Yun, and J. Zmuidzinas, Eds., vol. 5498, Oct. 2004, pp. 42–54.

[141] J. Dunkley, A. Amblard, C. Baccigalupi, M. Betoule, D. Chuss, A. Cooray, J. Delabrouille, C. Dickinson, G. Dobler, J. Dotson, H. K. Eriksen, D. Finkbeiner, D. Fixsen, P. Fosalba, A. Fraisse, C. Hirata, A. Kogut, J. Kristiansen, C. Lawrence, A. M. Magalhaes, M. A. Miville-Deschenes, S. Meyer, A. Miller, S. K. Naess, L. Page, H. V. Peiris, N. Phillips, E. Pierpaoli, G. Rocha, J. E. Vaillancourt, and L. Verde, "CMBPol Mission Concept Study: Prospects for polarized foreground removal," *ArXiv e-prints*, Nov. 2008.

[142] D. Samtleben and for the QUIET Collaboration, "Measuring the Cosmic Microwave Background Radiation (CMBR) polarization with QUIET," *ArXiv e-prints*, Feb. 2008.

[143] D. Benford and S. Moseley, "Cryogenic detectors for infrared astronomy: the Single Aperture Far-Infrared (SAFIR) Observatory," *Nucl. Instr. and Meth. A*, vol. 520, p. 379, 2004.

[144] D. Benford, S. Rinehart, D. Leisawitz, and T. Hyde, "Cryogenic Far-Infrared Detectors for the Space Infrared Interferometric Telescope (SPIRIT)," *Proc. SPIE*, vol. 6687, p. 66870E, 2007.

[145] J. C. Mather, "Cosmic background explorer (COBE) mission," in *Society of Photo-Optical Instrumentation Engineers (SPIE) Conference Series*, ser. Presented at the Society of Photo-Optical Instrumentation Engineers (SPIE) Conference, M. S. Scholl, Ed., vol. 2019, Oct. 1993, pp. 146–157.

[146] J. C. Mather, D. J. Fixsen, and R. A. Shafer, "Design for the COBE far-infrared absolute spectrophotometer (FIRAS)," in *Society of Photo-Optical Instrumentation Engineers (SPIE) Conference Series*, ser. Presented at the Society of Photo-Optical Instrumentation Engineers (SPIE) Conference, M. S. Scholl, Ed., vol. 2019, Oct. 1993, pp. 168–179.

[147] R. F. Silverberg, M. G. Hauser, N. W. Boggess, T. J. Kelsall, S. H. Moseley, and T. L. Murdock, "Design of the diffuse infrared background experiment (DIRBE) on COBE," in *Society of Photo-Optical Instrumentation Engineers (SPIE) Conference Series*, ser. Presented at the Society of Photo-Optical Instrumentation Engineers (SPIE) Conference, M. S. Scholl, Ed., vol. 2019, Oct. 1993, pp. 180–189.

[148] D. J. Fixsen, E. S. Cheng, D. A. Cottingham, W. C. Folz, C. A. Inman, M. S. Kowitt, S. S. Meyer, L. A. Page, J. L. Puchalla, J. E. Ruhl, and R. F. Silverberg, "A Balloon-borne Millimeter-Wave Telescope for Cosmic Microwave Background Anisotropy Measurements," *Ap.J.*, vol. 470, pp. 63–+, Oct. 1996.

[149] H. Murakami, J. Bock, M. M. Freund, H. Guo, T. Hirao, A. E. Lange, H. Matsuhara, T. Matsumoto, S. Matsuura, T. J. McMahon, M. Murakami, T. Nakagawa, M. Noda, K. Noguchi, H. Okuda, K. Okumura, T. Onaka, T. L. Roellig, S. Sato, H. Shibai, T. Tanabe, T. Watabe, T. Yagi, N. Yajima, and M. Yui, "The Infrared Telescope in Space (IRTS)," *Ap.J.*, vol. 428, pp. 354–362, Jun. 1994.

[150] B. P. Crill, P. A. R. Ade, D. R. Artusa, R. S. Bhatia, J. J. Bock, A. Boscaleri, P. Cardoni, S. E. Church, K. Coble, P. de Bernardis, G. de Troia, P. Farese, K. M. Ganga, M. Giacometti, C. V. Haynes, E. Hivon, V. V. Hristov, A. Iacoangeli, W. C. Jones, A. E. Lange, L. Martinis, S. Masi, P. V. Mason, P. D. Mauskopf, L. Miglio, T. Montroy, C. B. Netterfield, C. G. Paine, E. Pascale, F. Piacentini, G. Polenta, F. Pongetti, G. Romeo, J. E. Ruhl, F. Scaramuzzi, D. Sforna, and A. D. Turner, "BOOMERANG: A Balloon-borne Millimeter-Wave Telescope and Total Power Receiver for Mapping Anisotropy in the Cosmic Microwave Background," *Ap. J. Supp.*, vol. 148, pp. 527–541, Oct. 2003.

[151] S. Masi, P. A. R. Ade, J. J. Bock, J. R. Bond, J. Borrill, A. Boscaleri, P. Cabella, C. R. Contaldi, B. P. Crill, P. de Bernardis, G. de Gasperis, A. de Oliveira-Costa, G. de Troia, G. di Stefano, P. Ehlers, E. Hivon, V. Hristov, A. Iacoangeli, A. H. Jaffe, W. C. Jones, T. S. Kisner, A. E. Lange, C. J. MacTavish, C. Marini Bettolo, P. Mason, P. D. Mauskopf, T. E. Montroy, F. Nati, L. Nati, P. Natoli, C. B. Netterfield, E. Pascale, F. Piacentini, D. Pogosyan, G. Polenta, S. Prunet, S. Ricciardi, G. Romeo, J. E. Ruhl, P. Santini, M. Tegmark, E. Torbet, M. Veneziani, and N. Vittorio, "Instrument, method, brightness, and polarization maps from the 2003 flight of BOOMERanG," *Astron. Astrophy.*, vol. 458, pp. 687–716, Nov. 2006.

[152] P. L. Richards, M. Abroe, P. Ade, A. Balbi, J. Bock, J. Borrill, A. Boscaleri, P. de Bernardis, J. Collins, P. G. Ferreira, S. Hanany, V. V. Hristov, A. H. Jaffe, B. Johnson, A. T. Lee, T. Matsumu, P. D. Mauskopf, C. B. Netterfield, E. Pascale, B. Rabii, G. F.

Smoot, R. Stompor, C. D. Winant, and J. H. P. Wu, "The MAXIMA and MAXIPOL experiments," in *Experimental Cosmology at Millimetre Wavelengths*, ser. American Institute of Physics Conference Series, M. de Petris and M. Gervasi, Eds., vol. 616, May 2002, pp. 12–17.

[153] E. E. Haller, "Physics and design of advanced IR bolometers and photoconductors." *Infrared Physics*, vol. 25, pp. 257–266, 1985.

[154] J. Zhang, W. Cui, M. Juda, D. McCammon, R. L. Kelley, S. H. Moseley, C. K. Stahle, and A. E. Szymkowiak, "Hopping Conduction in Partially Compensated Silicon," *Phys. Rev. B*, vol. 48, p. 2312, 1993.

[155] ——, "Non-ohmic Effects in Hopping Conduction in Doped Silicon and Germanium between 0.05 - 1 Kelvin," *Phys. Rev. B*, vol. 57, p. 4472, 1998.

[156] B. Schulz, J. J. Bock, N. Lu, H. T. Nguyen, C. K. Xu, L. Zhang, C. D. Dowell, M. J. Griffin, G. T. Laurent, T. L. Lim, and B. M. Swinyard, "Noise performance of the Herschel-SPIRE bolometers during instrument ground tests," in *Society of Photo-Optical Instrumentation Engineers (SPIE) Conference Series*, ser. Presented at the Society of Photo-Optical Instrumentation Engineers (SPIE) Conference, vol. 7020, Aug. 2008.

[157] C. K. Stahle, M. D. Audley, K. R. Boyce, R. P. Brekosky, R. Fujimoto, K. C. Gendreau, J. D. Gygax, Y. Ishisaki, R. L. Kelley, R. A. McClanahan, T. Mihara, K. Mitsuda, S. H. Moseley, D. B. Mott, F. S. Porter, C. M. Stahle, and A. E. Szymkowiak, "Design and performance of the ASTRO-E/XRS microcalorimeter array and anticoincidence detector," in *Society of Photo-Optical Instrumentation Engineers (SPIE) Conference Series*, ser. Presented at the Society of Photo-Optical Instrumentation Engineers (SPIE) Conference, O. H. Siegmund and K. A. Flanagan, Eds., vol. 3765, Oct. 1999, pp. 128–136.

[158] N. Billot, P. Agnèse, J.-L. Auguères, A. Béguin, A. Bouère, O. Boulade, C. Cara, C. Cloué, E. Doumayrou, L. Duband, B. Horeau, I. le Mer, J. Lepennec, J. Martignac, K. Okumura, V. Revéret, M. Sauvage, F. Simoens, and L. Vigroux, "The Herschel/PACS 2560 bolometers imaging camera," in *Society of Photo-Optical Instrumentation Engineers (SPIE) Conference Series*, ser. Presented at the Society of Photo-Optical Instrumentation Engineers (SPIE) Conference, vol. 6265, Jul. 2006.

[159] P. K. Day, H. G. LeDuc, B. A. Mazin, A. Vayonakis, and J. Zmuidzinas, "A broadband superconducting detector suitable for use in large arrays," *Nature*, vol. 425, no. 6960, pp. 817–821, October 2003.

[160] B. A. Mazin, P. K. Day, J. Zmuidzinas, and H. G. LeDuc, "Multiplexable kinetic inductance detectors," *AIP Conference Proceedings*, no. 605, pp. 309–312, 2002.

[161] B. A. Mazin, P. K. Day, H. G. LeDuc, A. Vayonakis, and J. Zmuidzinas, "Superconducting kinetic inductance photon detectors," *Proceedings of the SPIE - The International Society for Optical Engineering*, vol. 4849, pp. 283–293, 2002.

[162] B. A. Mazin, "Microwave kinetic inductance detectors," Ph.D. dissertation, California Institute of Technology, Pasadena, CA 91125, August 2004.

[163] S. Kumar, "Submillimeter wave camera using a novel photon detector technology," Ph.D. dissertation, California Institute of Technology, Pasadena, CA 91125, 2008.

[164] J. Gao, "The physics of superconducting microwave resonators," Ph.D. dissertation, California Institute of Technology, Pasadena, CA 91125, 2008.

[165] J. S. Gao, J. Zmuidzinas, B. A. Mazin, H. G. LeDuc, and P. K. Day, "Noise properties of superconducting coplanar waveguide microwave resonators," *Applied Physics Letters*, vol. 90, no. 10, p. 102507, Mar 2007.

[166] J. Gao, J. Zmuidzinas, A. Vayonakis, P. Day, B. Mazin, and H. Leduc, "Equivalence of the effects on the complex conductivity of superconductor due to temperature change and external pair breaking," *Journal of Low Temperature Physics*, vol. 151, no. 1-2, pp. 557–563, April 2008.

[167] A. D. O'Connell, M. Ansmann, R. C. Bialczak, M. Hofheinz, N. Katz, E. Lucero, C. McKenney, M. Neeley, H. Wang, E. M. Weig, A. N. Cleland, and J. M. Martinis, "Microwave dielectric loss at single photon energies and millikelvin temperatures," *Applied Physics Letters*, vol. 92, no. 11, March 2008.

[168] J. J. Bock, A. Goldin, C. Hunt, A. E. Lange, H. G. LeDuc, P. K. Day, A. Vayonakis, and J. Zmuidzinas, "Integrated focal plane arrays for millimeter-wave astronomy," *AIP Conference Proceedings*, no. 605, pp. 243–246, 2002.

[169] A. Goldin, J. J. Bock, C. Hunt, A. E. Lange, H. LeDuc, A. Vayonakis, and J. Zmuidzinas, "SAMBA: superconducting antenna-coupled, multi-frequency, bolometric array," *AIP Conference Proceedings*, no. 605, pp. 251–254, 2002.

[170] A. Goldin, J. J. Bock, C. L. Hunt, A. E. Lange, H. G. LeDuc, A. Vayonakis, and J. Zmuidzinas, "Design of broadband filters and antennas for SAMBA," *Proceedings of the SPIE - The International Society for Optical Engineering*, vol. 4855, pp. 163–171, 2003.

[171] A. Goldin, J. J. Bock, A. E. Lange, H. LeDuc, A. Vayonakis, and J. Zmuidzinas, "Antennas for bolometric focal plane," *Nucl. Instrum. Meth. Phys. Res. A*, vol. 520, no. 1-3, pp. 390–392, March 2004.

[172] P. K. Day, H. G. Leduc, A. Goldin, T. Vayonakis, B. A. Mazin, S. Kumar, J. Gao, and J. Zmuidzinas, "Antenna-coupled microwave kinetic inductance detectors," *Nucl. Instrum. Meth. Phys. Res. A*, vol. 559, no. 2, pp. 561–563, Apr 2006.

[173] C. L. Kuo, P. Ade, J. J. Bock, P. Day, A. Goldin, S. Golwala, M. Halpern, G. Hilton, W. Holmes, V. Hristov, K. Irwin, W. C. Jones, M. Kenyon, A. E. Lange, H. G. LeDuc, C. MacTavish, T. Montroy, C. B. Netterfield, P. Rossinot, J. Ruhl, A. Vayonakis, G. Wang, M. Yun, and J. Zmuidzinas, "Antenna-coupled tes bolometers for the SPIDER experiment," *Nucl. Instrum. Meth. Phys. Res. A*, vol. 559, no. 2, pp. 608–610, Apr 2006.

[174] G. Chattopadhyay, C.-L. Kuo, P. Day, J. J. Bock, J. Zmuidzinas, and A. E. Lange, "Planar antenna arrays for CMB polarization detection," in *Proc. 2007 Joint 32nd International Conference on Infrared and Millimeter Waves and the 15th International Conference on Terahertz Electronics (IRMMW-THz)*, 2008, pp. 184–185.

[175] C. L. Hunt, J. J. Bock, P. K. Day, A. Goldin, A. E. Lange, H. G. LeDuc, A. Vayonakis, and J. Zmuidzinas, "Transition-edge superconducting antenna-coupled bolometer," *Proceedings of the SPIE - The International Society for Optical Engineering*, vol. 4855, pp. 318–321, 2003.

[176] M. Myers, W. Holzapfel, A. Lee, R. O'Brient, P. Richards, H. Tran, P. Ade, G. Engargiola, A. Smith, and H. Spieler, "An antenna-coupled bolometer with an integrated microstrip bandpass filter," *Applied Physics Letters*, vol. 86, no. 11, March 2005.

[177] M. Myers, P. Ade, G. Engargiola, W. Holzapfel, A. Lee, R. O'Brient, P. Richards, A. Smith, H. Spieler, and H. Tran, "Antenna-coupled bolometers for millimeter waves," *IEEE Transactions On Applied Superconductivity*, vol. 15, no. 2, pp. 564–566, June 2005.

[178] M. Myers, A. Peter, K. Arnold, G. Engargiola, B. Holzapfel, A. Lee, R. O'Brient, P. Richards, A. Smith, H. Spieler, and T. Huan, "Antenna-coupled bolometer arrays using transition-edge sensors," *Nucl. Instrum. Meth. Phys. Res. A*, vol. 559, no. 2, pp. 531–533, April 2006.

[179] M. J. Myers, K. Arnold, P. Ade, G. Engargiola, W. Holzapfel, A. T. Lee, X. Meng, R. O'Brient, P. L. Richards, H. Spieler, and H. T. Tran, "Antenna-coupled bolometer arrays for measurement of the cosmic microwave background polarization," *Journal of Low Temperature Physics*, vol. 151, no. 1-2, pp. 464–470, April 2008.

[180] R. O'Brient, P. A. R. Ade, K. Arnold, G. Engargiola, W. Holzapfel, A. T. Lee, M. J. Myers, X. F. Meng, E. Quealy, P. L. Richards, H. Spieler, and H. T. Tran, "A multi-band dual-polarized antenna-coupled tes bolometer," *Journal of Low Temperature Physics*, vol. 151, no. 1-2, pp. 459–463, April 2008.

[181] J. W. Kooi, G. Chattopadhyay, S. Withington, F. Rice, J. Zmuidzinas, C. Walker, and G. Yassin, "A full-height waveguide to thin-film microstrip transition with exceptional rf bandwidth and coupling efficiency," *Int. J. IR and MM Waves*, vol. 24, no. 3, pp. 261–284, March 2003.

[182] T. Stevenson, W. Hsieh, G. Schneider, D. Travers, N. Cao, E. Wollack, M. Limon, and A. Kogut, "Building blocks for a polarimeter-on-a-chip," *Nucl. Instrum. Meth. Phys. Res. A*, vol. 559, no. 2, pp. 611–613, April 2006.

[183] D. M. Glowacka, D. J. Goldie, S. Withington, M. Crane, V. Tsaneva, M. D. Audley, and A. Bunting, "A fabrication process for microstrip-coupled superconducting transition edge sensors giving highly reproducible device characteristics," *Journal of Low Temperature Physics*, vol. 151, no. 1-2, pp. 249–254, April 2008.

[184] D. J. Goldie, M. D. Audley, D. M. Glowacka, V. N. Tsaneva, and S. Withington, "Transition edge sensors for bolometric applications: responsivity and saturation," *Journal of Applied Physics*, vol. 103, no. 8, April 2008.

[185] T. Stevenson, D. Benford, C. Bennett, N. Cao, D. Chuss, K. Denis, W. Hsieh, A. Kogut, S. Moseley, J. Panek, G. Schneider, D. Travers, K. U-Yen, G. Voellmer, and E. Wollack, "Cosmic microwave background polarization detector with high efficiency, broad bandwidth, and highly symmetric coupling to transition edge sensor bolometers," *Journal of Low Temperature Physics*, vol. 151, no. 1-2, pp. 471–476, April 2008.

[186] S. J. C. Yates, J. J. A. Baselmans, R. Barends, Y. Lankwarden, H. F. Hoevers, J. Gao, T. Klapwijk, A. Neto, D. J. Bekers, G. Gerini, S. Doyle, P. D. Mauskopf, and P. Ade, "Antenna coupled kinetic inductance detectors for space based sub-mm astronomy," 2008, presented at the 2nd Workshop on the Physics and Applications of Superconducting Microresonators.

[187] S. Doyle, P. Mauskopf, J. Naylon, A. Porch, and C. Duncombe, "Lumped element kinetic inductance detectors," *Journal of Low Temperature Physics*, vol. 151, no. 1-2, pp. 530–536, April 2008.

[188] S. Doyle, "Kinetic inductance detectors," Ph.D. dissertation, Cardiff University, 2008.

[189] R. Barends, J. J. A. Baselmans, S. J. C. Yates, J. R. Gao, J. N. Hovenier, and T. M. Klapwijk, "Quasiparticle relaxation in optically excited high-Q superconducting resonators," *Physical Review Letters*, vol. 100, no. 25, June 2008.

[190] O. Noroozian, P. Day, J.-S. Gao, J. Glenn, S. Golwala, H. LeDuc, P.Maloney, B. Mazin, J. Sayers, J. Schlaerth, A. Vayonakis, and J.Zmuidzinas, "New resonator designs for reduced frequency noise in microwave kinetic inductance detectors (MKID)," 2008, presented at the 2nd Workshop on the Physics and Applications of Superconducting Microresonators.

[191] J. Baselmans, S. J. C. Yates, R. Barends, Y. J. Y. Lankwarden, J. R. Gao, H. Hoevers, and T. M. Klapwijk, "Noise and sensitivity of aluminum kinetic inductance detectors for sub-mm astronomy," *Journal of Low Temperature Physics*, vol. 151, no. 1-2, pp. 524–529, April 2008.

[192] J. Baselmans, S. Yates, R. Barends, J.-J. Lankwarden, J. Gao, H. F. Hoevers, and T. Klapwijk, "Optimizing kinetic inductance detectors for low background applications," June 19-20 2008, presented at the 2nd Workshop on the Physics and Applications of Superconducting Microresonators, SRON Utrecht.

[193] S. Weinreb, J. C. Bardin, and H. Mani, "Design of cryogenic SiGe low-noise amplifiers," *IEEE Transactions On Microwave Theory and Techniques*, vol. 55, no. 11, pp. 2306–2312, November 2007.

[194] T. K. Thrivikraman, J. Yuan, J. C. Bardin, H. Mani, S. D. Phillips, W.-M. L. Kuo, J. D. Cressler, and S. Weinreb, "SiGe HBT X-band LNAs for ultra-low-noise cryogenic receivers," *IEEE Microwave and Wireless Components Letters*, vol. 18, no. 7, pp. 476–478, July 2008.

[195] J. Gao, M. Daal, A. Vayonakis, S. Kumar, J. Zmuidzinas, B. Sadoulet, B. A. Mazin, P. K. Day, and H. G. Leduc, "Experimental evidence for a surface distribution of two-level systems in superconducting lithographed microwave resonators," *Applied Physics Letters*, vol. 92, no. 15, April 2008.

[196] J. Gao, M. Daal, J. M. Martinis, A. Vayonakis, J. Zmuidzinas, B. Sadoulet, B. A. Mazin, P. K. Day, and H. G. Leduc, "A semiempirical model for two-level system noise in superconducting microresonators," *Applied Physics Letters*, vol. 92, no. 21, May 2008.

[197] J. Schlaerth, A. Vayonakis, P. Day, J. Glenn, J. Gao, S. Golwala, S. Kumar, H. LeDuc, B. Mazin, J. Vaillancourt, and J. Zmuidzinas, "A millimeter and submillimeter kinetic inductance detector camera," *Journal of Low Temperature Physics*, vol. 151, no. 3-4, pp. 684–689, May 2008.

[198] B. A. Mazin, P. K. Day, K. D. Irwin, C. D. Reintsema, and J. Zmuidzinas, "Digital readouts for large microwave low-temperature detector arrays," *Nucl. Instrum. Meth. Phys. Res. A*, vol. 559, no. 2, pp. 799–801, April 2006.

[199] C. Muirhead, J. Healey, and M. Colclough, "Magnetic field tuning of coplanar waveguide resonators," 2008, presented at the 2nd Workshop on the Physics and Applications of Superconducting Microresonators.